Geoscience Frontiers 9 (2018) 1777–1794

HOSTED BY

Contents lists available at ScienceDirect

China University of Geosciences (Beijing)

Geoscience Frontiers

journal homepage: www.elsevier.com/locate/gsf

Research Paper

On the radiogenic heat production of metamorphic, igneous, and sedimentary rocks

D. Hasterok [a,b,*], M. Gard [a], J. Webb [a,c]

[a] Department of Earth Sciences, University of Adelaide, North Terrace, SA, 5005, Australia
[b] Centre for Tectonics Research and Exploration (TRaX), University of Adelaide, North Terrace, SA, 5005, Australia
[c] Ramelius Resources Ltd., East Perth, WA 6005, Australia

ARTICLE INFO

Article history:
Received 1 June 2017
Received in revised form
6 September 2017
Accepted 24 October 2017
Available online 13 November 2017
Handling Editor: Christopher Spencer

Keywords:
Heat generation
Density
Metamorphic rocks
Sedimentary rocks
Igneous rocks
Continental lithosphere

ABSTRACT

Sedimentary rocks cover ~73% of the Earth's surface and metamorphic rocks account for approximately 91% of the crust by volume. Understanding the average behavior and variability of heat production for these rock types are vitally important for developing accurate models of lithospheric temperature. We analyze the heat production of ~204,000 whole rock geochemical data to quantify how heat production of these rocks varies with respect to chemistry and their evolution during metamorphism. The heat production of metaigneous and metasedimentary rocks are similar to their respective protoliths. Igneous and metaigneous samples increase in heat production with increasing SiO_2 and K_2O, but decrease with increasing FeO, MgO and CaO. Sedimentary and metasedimentary rocks increase in heat production with increasing Al_2O_3, FeO, TiO_2, and K_2O but decrease with increasing CaO. For both igneous and sedimentary rocks, the heat production variations are largely correlated with processes that affect K_2O concentration and covary with other major oxides as a consequence. Among sedimentary rocks, aluminous shales are the highest heat producing (2.9 $\mu W\ m^{-3}$) whereas more common iron shales are lower heat producing (1.7 $\mu W\ m^{-3}$). Pure quartzites and carbonates are the lowest heat producing sedimentary rocks. Globally, there is little definitive evidence for a decrease in heat production with increasing metamorphic grade. However, there remains the need for high resolution studies of heat production variations within individual protoliths that vary in metamorphic grade. These results improve estimates of heat production and natural variability of rocks that will allow for more accurate temperature models of the lithosphere.

1. Introduction

Many solid Earth processes and properties are dependent upon temperature or the relative temperature differences within the lithosphere (Sandiford et al., 2001; Kelsey and Hand, 2015; McKenzie and Priestley, 2016). Accurately estimating lithospheric temperatures and uncertainties is difficult without reliable estimates of heat production. Many studies (e.g., Sizova et al., 2015; Jeanniot et al., 2016; Liu and Currie, 2016), particularly geodynamic models, assume values for lithospheric heat production using global or lithospheric averages for the upper crust and lower crust that are more than 30 years old (e.g., Taylor and McLennan, 1985). The most accurate models are tailored to observations of heat production on rocks within the same terrane or geologic province (e.g. McLaren et al., 2006). For many regions, a sufficiently large dataset may not exist to produce precise estimates. For these regions, an improved set of global estimates tailored to specific rock types are desired for placing realistic bounds on temperature.

Hasterok and Webb (2017) used a global geochemical database to estimate the heat production of igneous rocks. However, sedimentary rocks account for 73% of exposed continental rocks (Fig. 1; Wilkinson et al., 2009). While sediment thicknesses can exceed 10 km in some cases (Laske and Masters, 1997), only 4% of the continental crust may be sedimentary by volume (Wilkinson et al.,

* Corresponding author. Department of Earth Sciences, University of Adelaide, North Terrace, SA, 5005, Australia.
E-mail addresses: dhasterok@gmail.com (D. Hasterok), matthew.gard@adelaide.edu.au (M. Gard).
Peer-review under responsibility of China University of Geosciences (Beijing).

https://doi.org/10.1016/j.gsf.2017.10.012

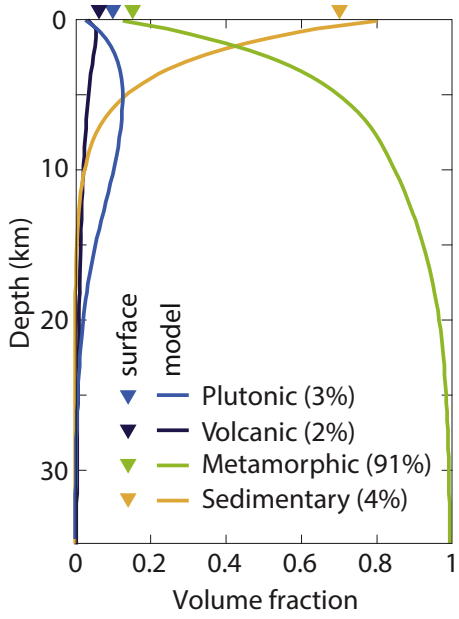

Figure 1. Estimated percentages of continental crust by rock group/origin (modified from Wilkinson et al., 2009). Triangles indicate percentages of surface exposures determined from geologic maps. Lines are estimates derived from models of crustal cycling.

2009). Metamorphic rocks may represent a far greater proportion of the continental crust, roughly 91% by volume (Wilkinson et al., 2009). Although presumably most of the 91% is of igneous (plutonic) origins due to the increased likelihood of increased preservation as a function of increasing depth of formation. Therefore, an understanding of the crustal heat production is incomplete without reliable constraints on how heat production is changed through the process of metamorphosing sedimentary and igneous rocks.

This study aims to quantify the heat production of sedimentary and metamorphic rocks and describe this variation with chemistry and metamorphic grade. To estimate the heat production distributions, we compile and analyze a global geochemical database with >204,000 whole-rock major and trace element analyses. We show that the heat production of a metamorphic rock is controlled by the original protolith and that patterns emerging from the set of igneous and sedimentary rocks exhibit fundamentally different behaviors with respect to major element concentrations, and neither show a definitive decrease in heat production with metamorphic grade.

2. Geochemical datasets

2.1. Sources

We compiled >800,000 whole rock major and trace element data from a combination of online databases, government reports, and >500 journal papers (Table 1). Most of the data (611,200) are derived from EarthChem and associated databases (Fig. 2a); only 120,340 of which are suitable for estimating of heat production. Our additions focus on metamorphic and sedimentary samples as well as regions sparsely covered by EarthChem (Fig. 2b). Approximately 25% (~204,000) of the samples in this database include the necessary chemical analyses to estimate both density and heat production (Table 1). Most of the analyses in this database are igneous and were previously described by Hasterok and Webb (2017) although a few have been reclassified as metaigneous on the basis of their descriptions. About 9% of the dataset is sedimentary with slightly fewer metamorphic analyses. Nearly half the metamorphic data include sufficient descriptions that igneous and sedimentary protoliths may be identified.

Table 1
Number of data for which heat production can be computed or estimated.

Rock group	With HPE	Estimated U	Estimated Th	Total
Igneous	117,304	41,563	3753	162,620
All metamorphic	16,824	1598	374	18,796
Metaigneous	4852	1125	254	6231
Metasedimentary	3765	478	122	4365
Sedimentary	12,269	3867	887	17,023
Total	146,397	47,033	5016	198,446

It is quite likely that many of the rocks labeled as igneous and sedimentary are metamorphic in nature, but their descriptions are insufficient to identify them as such. We base this on a survey of papers contained within the database. In some cases, descriptions of samples provided in the original reference indicate metamorphism, but names provided in published tables and transferred to the database were derived from the unmetamorphosed protolith. It is uncertain how large an impact, if at all, this distinction will have on our observations.

2.2. Chemical classification of samples

Nomenclature presents a significant challenge when analyzing these large databases. Naming schemes are diverse and may be based on textural characteristics and/or grain size, mineralogy and/or thermodynamic conditions, in addition to chemistry. Among chemical systems, there are a number of different schemes, some with nomenclature which intersect, but are not identical sets. Furthermore, the names assigned by authors may not be based upon a rigorous examination of the chemistry, but are instead based on field descriptions or derived from named map units that may not be homogeneous in composition. For example, quartzites which are typically classified as having >90% modal quartz include samples in the global dataset with SiO_2 as low as 10 wt.%. Unfortunately, these gross misclassifications are not isolated occurrences as the quartzite designation appears to be more or less continuously applied to any sedimentary rock regardless of its SiO_2 concentration, albeit decreasing in frequency as SiO_2 decreases.

Therefore, we seek a more uniform system to classify samples within the database. We use separate chemical classification systems depending upon whether the rocks originates from igneous or sedimentary protoliths. For metamorphic rocks, we include additional fields based on the metamorphic facies and/or texture when possible. Because we employ a hierarchical naming scheme, we are able to retain knowledge of metamorphism despite using unmetamorphosed names.

Different studies report different sets of major oxides, with or without volatiles. As a result, we seek a consistent scheme that can be uniformly applied to the entire database. We normalize to a volatile-free composition using the following set of oxides: SiO_2, TiO_2, Al_2O_3, Cr_2O_3, FeO^t, MgO, MnO, NiO, CaO, Na_2O, K_2O, P_2O_5, and BaO. While not all analyses report each of these as major oxides, in many cases the data are included in trace element lists and can be used to compute oxide concentrations (e.g., NiO as Ni). While normalizing the data can result in a change in classification of the rock type, the changes are typically minor, limited to crossing chemical adjacent boundaries. Because rock compositions form a continuum (Fig. 3) a slight change in the name has negligible impact on our results and interpretation.

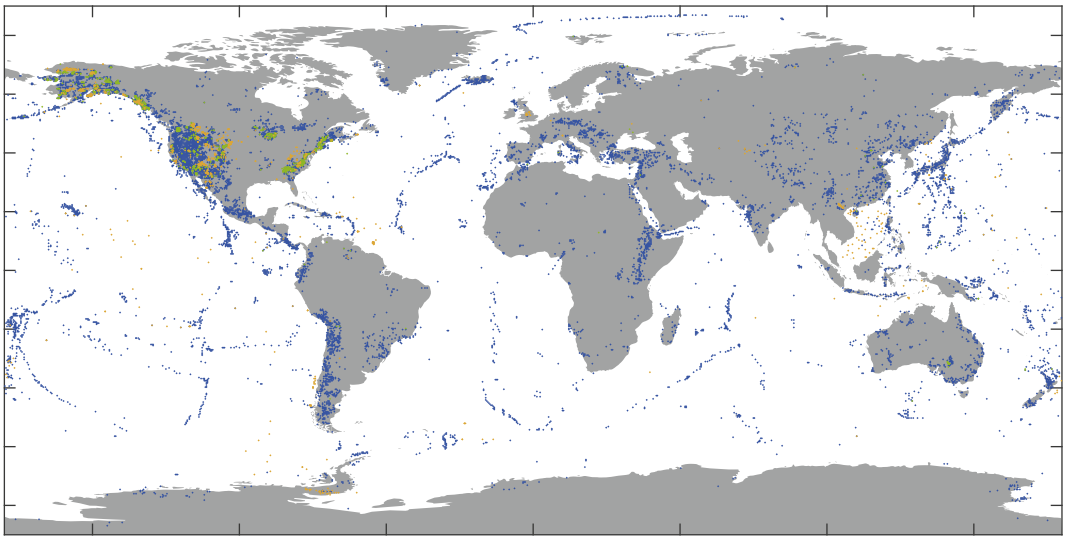

(a) EarthChem.org (120,340)

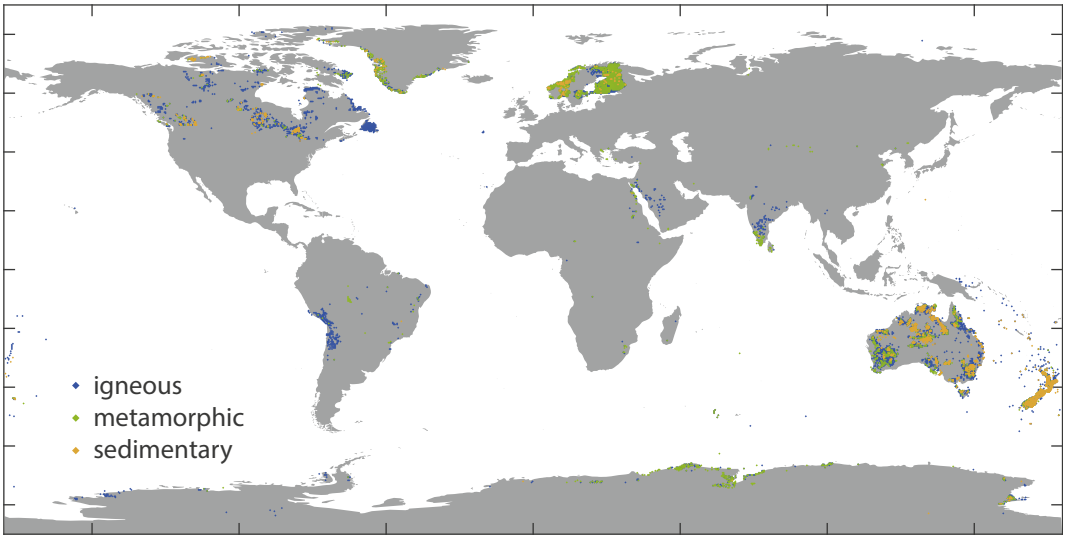

(b) this study (83,774)

Figure 2. Locations of samples for which heat production is estimated. Data from (a) the EarthChem portal and (b) supplemental sources in this article. A list of references are included in the supplementary material.

2.2.1. Igneous and metaigneous classification

To classify igneous rocks, we use a total alkali-silica (TAS) classification scheme (Middlemost, 1994) that has been slightly modified to include additional fields for high-Mg volcanics (Le Bas and Streckeisen, 1991). We also attempt to separate plutonic cumulates from mantle peridotites on the basis of magnesium number (>80 for mantle peridotites). We classify igneous rocks as carbonatites when the CO_2 concentration exceeds 20 wt.%; which includes some carbonated silicates and CO_2 altered basalts.

For many metaigneous rocks, it is difficult to determine whether they are intrusive or extrusive on the basis of the names or descriptions included in the database. Because plutonic and volcanic rocks behave in quite similar ways chemically (including heat production, Hasterok and Webb, 2017), we combine the analysis of the two for this study.

2.2.2. Sedimentary and metasedimentary classification

To classify sedimentary rocks, we combine two chemical classification methods. The first method is akin to the quartz-feldspar-lithics (QFL) scheme. We use the ternary SiO_2, $Al_2O_3 + Fe_2O_3$, and $CaO + MgO$ system (Mason, 1952; Turekian, 1969). This scheme allows us to separate carbonates and soils from the more clastic sediments. We then use the method by Herron (1988) to further classify clastic sediments which examines the ratios of SiO_2/Al_2O_3 and Fe_2O_3/K_2O in log-space. We retain quartzites as a special case in the ternary system where SiO_2 exceeds 0.9.

2.2.3. Metamorphic classification

Typical classification schemes for metamorphic rocks are built on three fundamentally different characteristics: the mineralogic or chemical composition, texture, and/or facies. The names ascribed to the individual samples vary from low information content (e.g., gneiss and schist) to high information content (e.g., hornblende biotite gneiss and amphibolitized tholeiite dyke). In many cases a rock may be simply identified as metamorphic.

Lacking complete descriptions of samples within the database, we divide samples based on the descriptions provided into a simplified set of names that we can use to examine patterns of heat

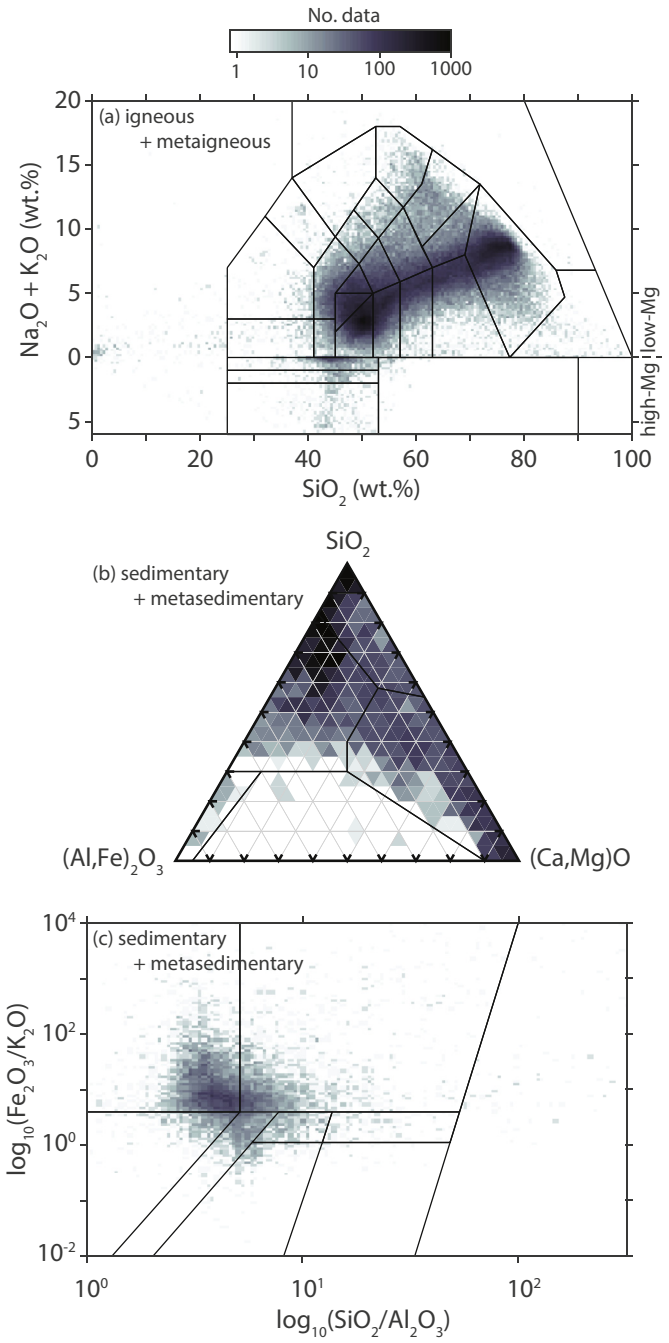

Figure 3. Number of data in relation to classification schemes used in this study. (a) TAS scheme (Le Bas and Streckeisen, 1991; Middlemost, 1994). Modified to show high-Mg volcanics as values positive alkali below the zero line. Additional fields have been added to separate cumulate from mantle peridotites and further separate foidolite fields. (b) Classification scheme for sedimentary and metasedimentary samples (modified from Mason, 1952; Turekian, 1969). (c) Additional classification of psammitic and pelitic sample samples (Herron, 1988).

production. The set of metamorphic facies and textures used in this study are listed in Table 3. To ascribe these terms to the samples, we search the names and descriptions for patterns related to these facies. For example, to identify a schist, we search for the following patterns within the names and descriptions: schist, greenschist, blueschist, and schistose.

In some cases an approximate metamorphic facies can be determined from the given name. Metamorphic textural names also provide a clue as to the general metamorphic grade. For example, granulite represents both a texture and a facies. While the term is typically reserved for rocks of granulite facies, it need not be the case. Schist is another very common textural description, which may apply to blue- or greenschist facies but is also commonly used to describe samples of amphibolite facies. Gneiss is typically applied to rocks that have experienced amphibolite or granulite conditions.

However imprecise, we can use these groupings to investigate the general variations in global heat production as a function of metamorphic grade. We have ordered the names and textures in Table 3 to indicate our general assumptions about metamorphic grade based on names and descriptions provided with the samples.

Not all metamorphic rocks that we assign a metamorphic grade and/or texture can be used in this study because the protolith type is unknown. If there were a way to accurately estimate the protolith from chemistry a significantly greater number of samples could be included (Table 3).

3. Methods

3.1. Heat production, A

Heat production is determined from the chemical composition with the relationship

$$A\left(\mu W\ m^{-3}\right) = \rho(9.67C_U + 2.56C_{Th} + 2.89C_{K_2O}) \times 10^{-5} \quad (1)$$

with concentrations, C, of heat producing elements (HPEs) in parts per million (ppm) except K_2O in weight percent (wt.%), and density, ρ, in kg m^{-3} (Rybach, 1988).

3.2. Density, ρ

Only a small fraction of the dataset have density observations reported with chemical analyses. The global geochemical database includes several datasets with density observations that we use to develop an oxide-based model (Haus and Pauk, 2010; Barette et al., 2016; Bédard et al., 2016; Slagstad, 2008, 2017). Most of the density data range from 2400 to 3500 kg m^{-3}.

The density data fall into four groups that can be separated on the basis of composition: low-MgO silicate-dominated rocks; high-MgO silicate-dominated rocks; igneous carbonatites/carbonated silicate rocks; and carbonate-dominated sedimentary rocks (Fig. 4). A single density formula cannot be used to provide an estimate for all of these rock types.

To develop models for density, we use multiple linear regression using oxides and/or geochemical indices. In addition to seeking the lowest misfit, our goal is to minimize the number of oxides used in the estimate so that the number of samples available for computation may be maximized since complete chemical analyses are not always reported (particularly for carbonates and carbonatites).

Coefficients for the linear regression models are given in Table 2. Aside from low-MgO rocks, major oxides were found to produce the most reliable estimates of density (Table 2). For low-MgO rocks, geochemical indices are used to compute the density model because they are less sensitive to geochemical variability and provide a more stable estimate of the density when incomplete geochemical analyses are provided. We use the following geochemical indices in to estimate our low-MgO density model,

$$Fe^* \text{ (iron number)} = C_{FeO^t}\left(C_{FeO^t} + C_{MgO}\right)^{-1}$$

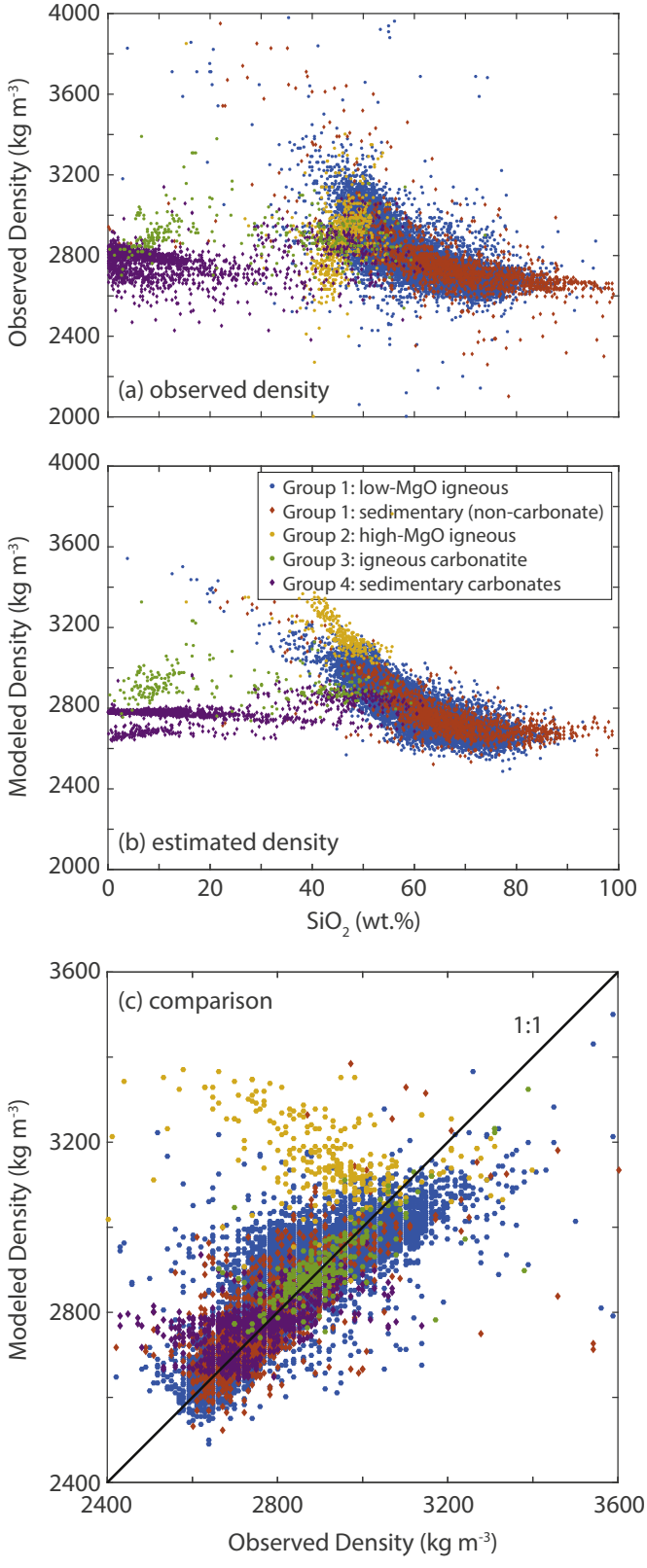

Figure 4. Observed (a) and modeled (b) density for four distinct chemical sets. Comparison of models are shown in (c). Density of high-magnesium data are estimated using the same model as the low-magnesium rocks. While a model that matches these data can be constructed, we prefer to use the low-magnesium model (see Section 3.2 for details).

Table 2
Density models and their uncertainty for compositional groups.

Model	Low-Mg silicates		High-Mg silicates	Igneous carbonatite	Sedimentary carbonate
No. of data	15,973	18,019	627	264	1740
RMS misfit (kg m^{-3})	82	91	154	69	144
Parameter[a]					
ρ_0	2561 ± 10	2532 ± 10	3143 ± 83	2733 ± 21	3402 ± 189
Fe*	196 ± 12	216 ± 12			
Maficity	662 ± 14	608 ± 15			
MALI	−10.3 ± 0.3	−10.0 ± 0.3			
LOI	−10.0 ± 0.4				
SiO_2					−8.0 ± 2.5
MgO			−10.6 ± 2.2		−4.5 ± 1.8
CaO			6.2 ± 4		−7.6 ± 1.8
FeO^t				13.6 ± 1.5	
P_2O_5				8.8 2.3	

[a] Values are reported with ±2σ.

Table 3
Number of metamorphic rocks with heat production analyses by facies and/or texture, ordered ascending from low to high grade.

	Facies	Protolith		Total[a]
		Igneous	Sedimentary	
Low grade	Zeolite	3	0	3
	Hornfels	43	215	374
	Phrenite	0	346	387
	Slate[b]	0	289	289
	Schist[b,c]	264	1223	3563
	Amphibolite	801	39	1938
	Gneiss[b]	2590	214	5804
	Migmatite[b]	116	22	594
	Granulite	469	39	1125
High grade	Eclogite	56	0	148

[a] Includes unclassified protoliths.
[b] Indicates textural name rather than facies.
[c] Includes blue- and greenschist.

$$\text{MALI (modified alkali-lime index)} = C_{Na_2O} + C_{K_2O} - C_{CaO}$$

$$\text{maficity} = n_{Fe} + n_{Mg} + n_{Ti}$$

where n is the number of moles of each specified oxide component and FeO^t is the total iron. Density estimates <2400 and >3600 kg m^{-3} are removed to limit the influence of extreme outliers.

The high-MgO igneous rocks include boninites, komatiites, picrites, mantle peridotites, and cumulate peridotites. The low-MgO density model predicts a density of 3364 kg m^{-3} for mantle peridotites whereas the high-MgO density model predicts a median density of 2640 kg m^{-3}. While the latter is consistent with the observed data in this database, the former is consistent with studies of fresh peridotites (e.g., Boyd and McCallister, 1976; Christensen and Mooney, 1995). The disparity between low observed densities and typically high published values for high-MgO rock types is not limited to peridotite, but common among all of these rocks.

The low densities observed within this dataset may be a result of serpentinization or other forms of hydrous alteration that can reduce densities by several hundred kg m^{-3} (Toft et al., 1990). As olivine is a common mineral in high-MgO silicate-dominated rocks, we assume that its alteration to serpentinite is the cause of the low observed densities among these rock types. Regardless the values are too low to be realistic for fresh samples of similar compositions, hence we prefer the low-MgO density model estimate the density of high-MgO compositions (Fig. 4b).

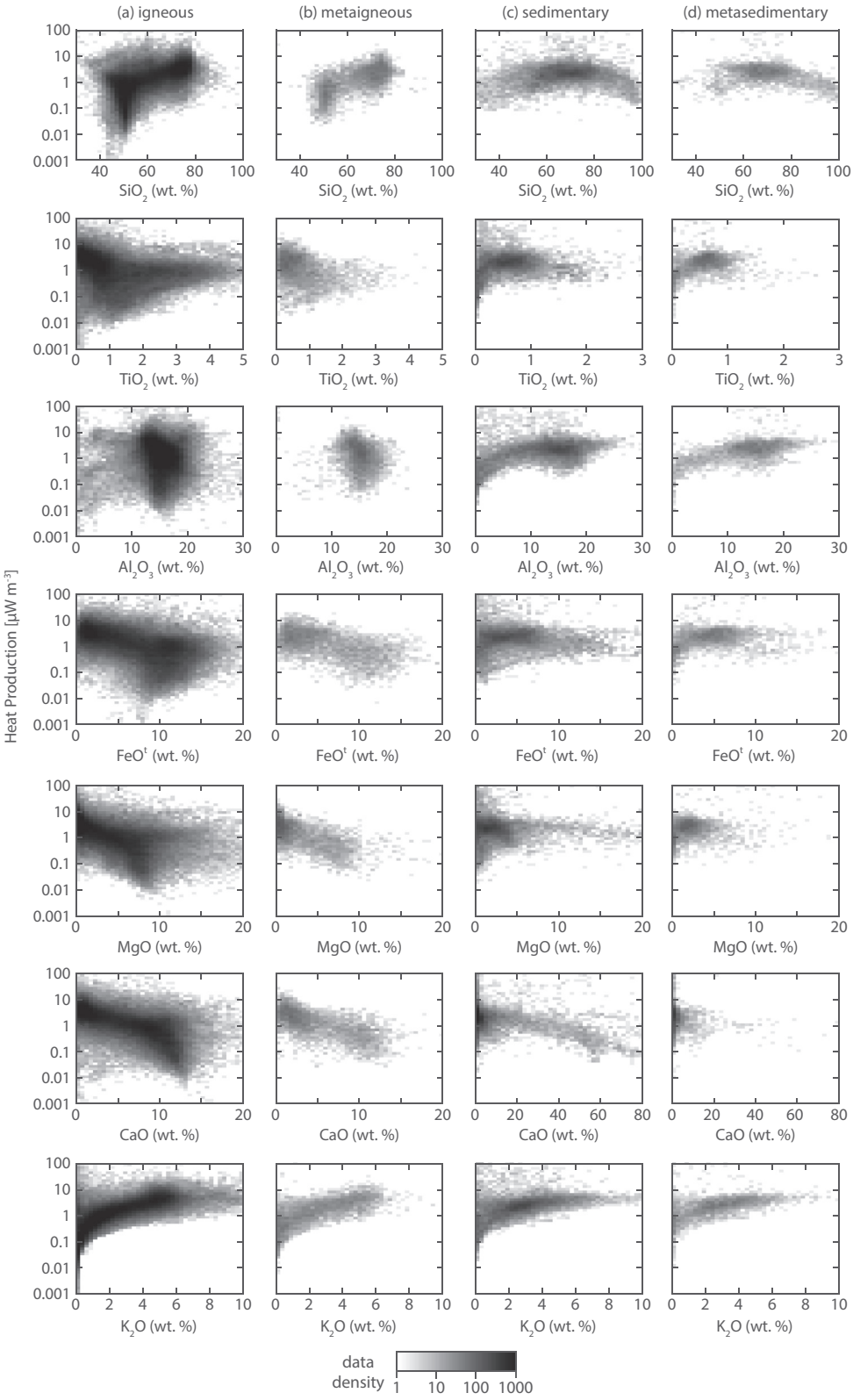

Figure 5. Heat production as a function of selected major oxides for samples identified as (a) igneous, (b) metaigneous, (c) sedimentary and (d) metasedimentary samples. The data are presented as two dimensional histograms with a logarithmic color scheme indicating the quantity in each bin.

Our density models are computed on an anhydrous basis; however, inclusion of a loss on ignition (LOI) term improves density estimates slightly for low-MgO rocks (Table 2). Including an LOI term reduces misfit by 9 kg m^{-3} (~10%), but has a small influence on heat production estimates which are dominated by changes in HPE concentrations. LOI is only reported for approximately half the samples for which we can estimate heat production. Therefore, we do not include an LOI term in our density computation to provide a consistent basis upon which to compare the data.

We prefer to have a near zero porosity for developing our geochemical estimates of density for two reasons. First, it provides a basis for common comparison between rock types free from non-compositional related effects. Second, our models provide an upper bound for density and heat production that can be easily adjusted to individual samples if the porosity is known.

Porosity variations will add variability that cannot be accounted for by chemistry; however, porosity determinations are not included in this dataset. While sedimentary rocks can reach porosities >30%, resulting in dramatic reductions to density, we assume most of the samples in this database are near zero porosity. We base this assumption on the similar distribution of sedimentary rocks to igneous samples with similar SiO_2 concentrations (Fig. 4). With the exception of samples from Barette et al. (2016), most samples are from Precambrian terranes that have generally experienced some level of metamorphism and hence are likely low porosity.

4. Data treatment

4.1. Censored data

When an attempt to determine the concentration of an element is made, but the exact value is unknown, the datum is said to be censored. There are three types of censoring that can occur when measuring geochemical data: left censored, data that fall below the detection limit; right censored, data that are above a maximum recordable value; and interval censored, data that are rounded. Very few geochemical data are right censored, so in this case we assume the value is equivalent to the maximum recordable value with little bias on the overall distribution. However, there may be an effect on the heat production estimates due to left and interval censoring, which are far more common.

4.1.1. Interval censored data

Interval censoring of geochemical data is very common as many data are rounded to the nearest 0.01, 0.1, 1, or 10 ppm. The effect of interval censoring is obvious in histograms of observed U and Th data, resulting in a comb-like appearance of peaks in the distribution (Fig. 7). When the data are interval censored, a reported value of 4 ppm may actually fall anywhere within the interval from 3.5 to 4.5 ppm. Since the distributions of heat producing elements are more log-normal than Gaussian, observations that fall below the median may be biased towards lower concentrations and observations above the median value may be biased towards higher concentrations. However, the effect of interval censoring on our data may be minimal since the range of concentrations varies by several orders of magnitude and the level of interval censoring varies, i.e. some data are reported to one or two decimal places other than rounded to the nearest ppm. Therefore, we do not attempt to correct for the influence of interval censoring.

4.1.2. Left censored data

Left censored data are more common for elements that are typically found in low concentrations. U, and less commonly Th, fall below the reported detection limit, which varies from study to study. Some studies report U concentrations below 0.01 ppm, while others may report values falling below a detection limit of 10 ppm. Left censoring can make it difficult to accurately determine the average heat production for a rock type when a significant fraction of the data fall below the detection limit. Simply assuming a value of zero will result in biasing the distribution towards lower values. Assuming a value at the detection limit will bias the distribution towards high values. Taking a value half-way between 0 and the detection limit will also bias the estimated distribution (Helsel, 2004). Ignoring the data will bias the resulting distribution towards higher values as fewer low values are included.

Although there are statistical methods for improving estimates of the true sampled distribution in the case of left censoring (Helsel, 2004), we prefer to use a simpler approach that takes into account additional information provided through the use of multi-element analyses that have become routine. For instance, it is well known that Th and U are highly correlated (Taylor and McLennan, 1985), which we can exploit to estimate the concentration of an element below detection when the other is above detection.

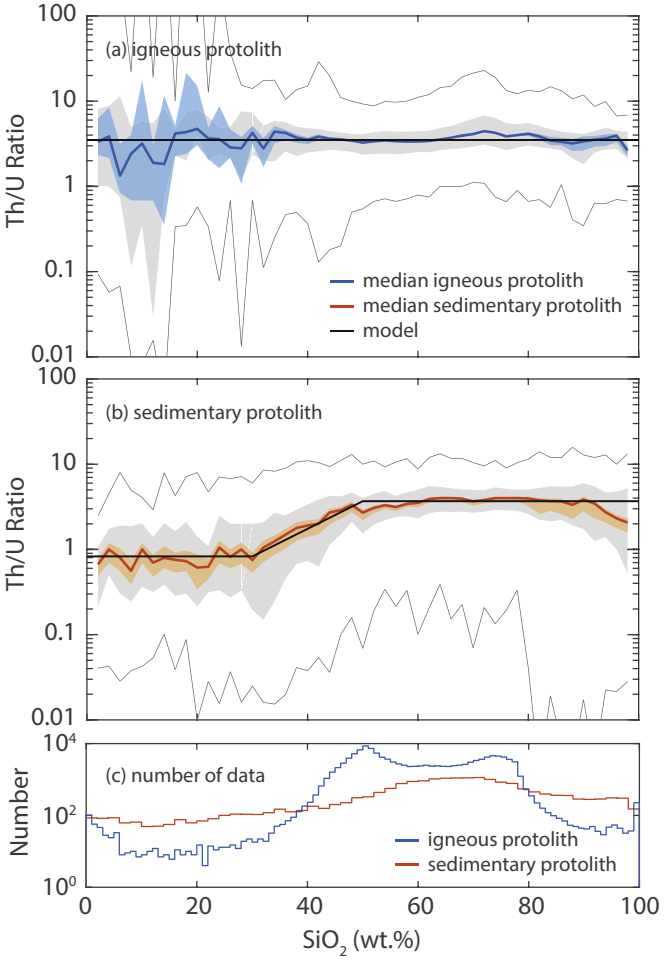

Figure 6. The Th/U ratio as a function of SiO_2 concentration for (a) igneous and metaigneous samples, and (b) sedimentary and metasedimentary samples. The 0.025 and 0.975 quantiles are indicated by the gray lines, the 0.25 and 0.75 quantiles are the boundaries of the filled gray region, and the 0.5 quartile is indicated by the heavy colored line. The colored patches approximate the 95% confidence bound on the median. The heavy black line indicates our modeled Th/U ratio for each of the datasets as a function of SiO_2 content. The number of analyses used to estimate the averages are found in (c).

4.1.3. Estimating U and Th concentrations

There are several trace elements that are highly correlated with U and Th in log-space, including Rb, La, and Ce. However, the highest correlation occurs between U and Th (~0.86).

The distribution of Th/U ratio is well-behaved for SiO_2 >50 wt.%, but <30 wt.% the distribution broadens considerably for both igneous and sedimentary rocks. For igneous rocks, the average Th/U ratio falls between 3 and 4 for most values of SiO_2 in spite of the larger variability for rocks with low silica (Fig. 6). For sedimentary rock, the estimated radiogenic heat production for low silica (<30 wt.%), generally carbonates, have considerably lower Th/U ratios (Fig. 6). Between 30 wt.% and 50 wt.% the variation in the

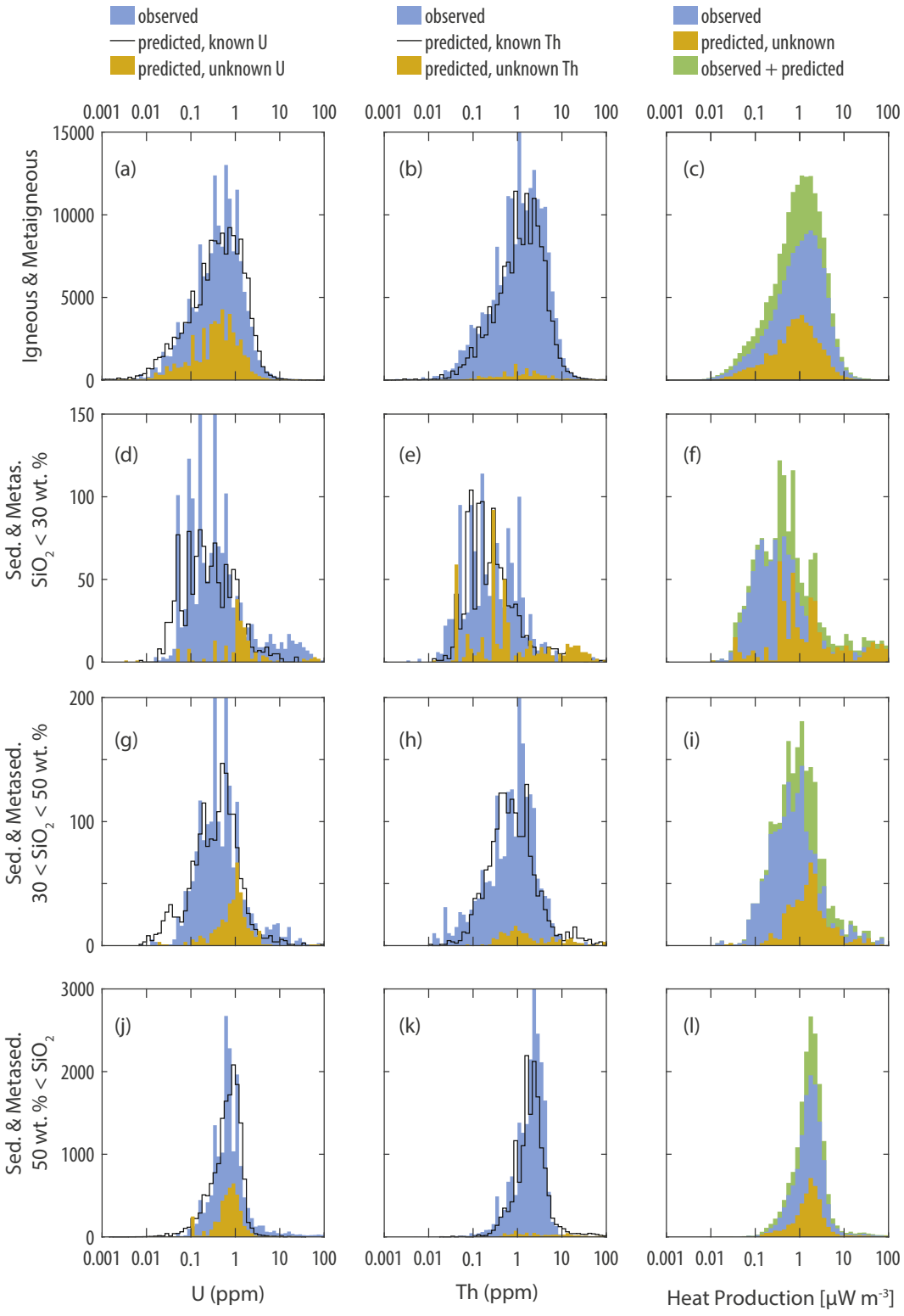

Figure 7. Heat production estimated by predicting U or Th concentrations from the U/Th ratio.

Th/U ratio varies nearly linearly between the carbonate and siliciclastic ratios due to mixing of carbonate and siliciclastic components.

There is a slight increase in the Th/U ratio from mafic to felsic compositions (Fig. 6a). A similar trend in Th/U was previously noted in igneous zircons derived from a range of mafic to felsic samples (Kirkland et al., 2015). While this trend is statistically significant the variation is relatively small with respect to the natural variability. Therefore, a constant value will provide a reasonable estimate for the U or Th concentration without significantly skewing the distributions.

The average Th/U ratio determined from this dataset is lower than previous estimates for the average Th/U ratio of surface rocks. For igneous rocks, the median Th/U ratio is 3.53 with log-normal scale parameters $(\mu, \sigma) = (1.26, 0.75)$, which represent the mean and standard deviation in ln-space. For sedimentary rocks, siliciclastics have a median Th/U ratio of 3.68 with scale parameters (1.30, 1.17) and carbonates have a median Th/U ratio of 0.84 with scale parameters (−0.176, 1.34). The number of igneous and metaigneous data used to calibrate the Th/U ratio is 153,020 and for sedimentary and metasedimentary rocks the numbers are 15,954 and 1175 for siliciclastics and carbonates, respectively.

The average Th/U ratios determined from this database are lower than previously reported averages for surface samples, although not outside quoted uncertainties (e.g., 3.9 ± 0.4; McDonough and Arevalo, 2008).

By using Th/U to predict left censored or otherwise unreported concentrations of U and Th, we increase the number of samples that can be analyzed by ~26% (Table 1). Most of the estimated data are U values, which is unsurprising for two reasons. Both elements are often reported to the same level of detection and U is typically

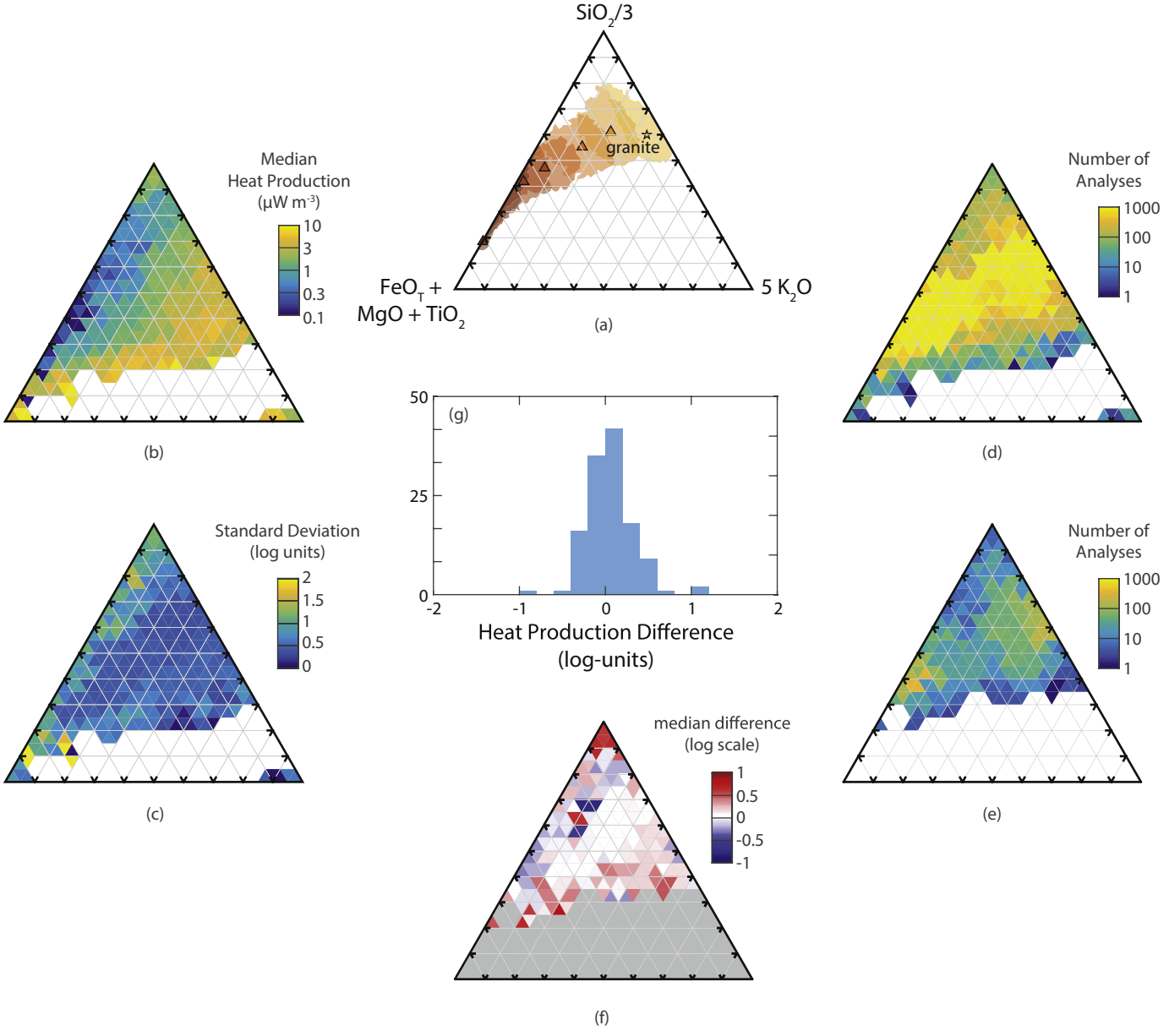

Figure 8. Variations in igneous and metaigneous heat production with silicic content, maficity and potassium. Ternary diagrams are computed in molar fraction. (a) Median points and contours encompassing 90% of subalkaline plutonic rocks defined by the TAS classification (Middlemost, 1994). Samples progress from granite to peridotgabbro. (b) Median heat production and (c) standard deviation ($\log_{10}$ units) for combined igneous and metaigneous samples. Number of (d) igneous and (e) metaigneous samples. (f) Difference between $\log_{10}$ mean of heat production between igneous and metaigneous samples. (g) Histogram of the difference in means.

lower than Th, making U more likely to fall below detection. In addition, publications prior to the late 1990s often included Th as part of trace element analyses but rarely U due to the difficulty and cost involved in obtaining reliable U estimates.

Using Th to estimate U and vice versa when both elements are above detection limits reasonably reproduces each element's observed distribution for igneous rocks and siliciclastic sedimentary rocks. The RMS misfit between the known and estimated distributions are 0.32 and 0.51 $\log_{10}$ units for igneous and high SiO_2 sedimentary protoliths, respectively. The estimates are less accurate (RMS = 0.59) for intermediate and low (RMS = 0.61) SiO_2 sedimentary rocks due to the broader distributions of the Th/U ratios, but there is no apparent shift in the median.

The distributions of data where Th or U are unknown are relatively similar to the distributions of known data for igneous and sedimentary siliciclastic protoliths. Sedimentary protoliths with low to intermediate SiO_2 typically have higher heat production distributions for the estimated U and Th data than the observed distributions. Perhaps this difference indicates an undersampling of sedimentary protoliths with these compositions. Regardless, for a majority of rock samples, estimation of Th or U using Th/U ratios provide a reasonable estimate of for left censored and elements not analyzed.

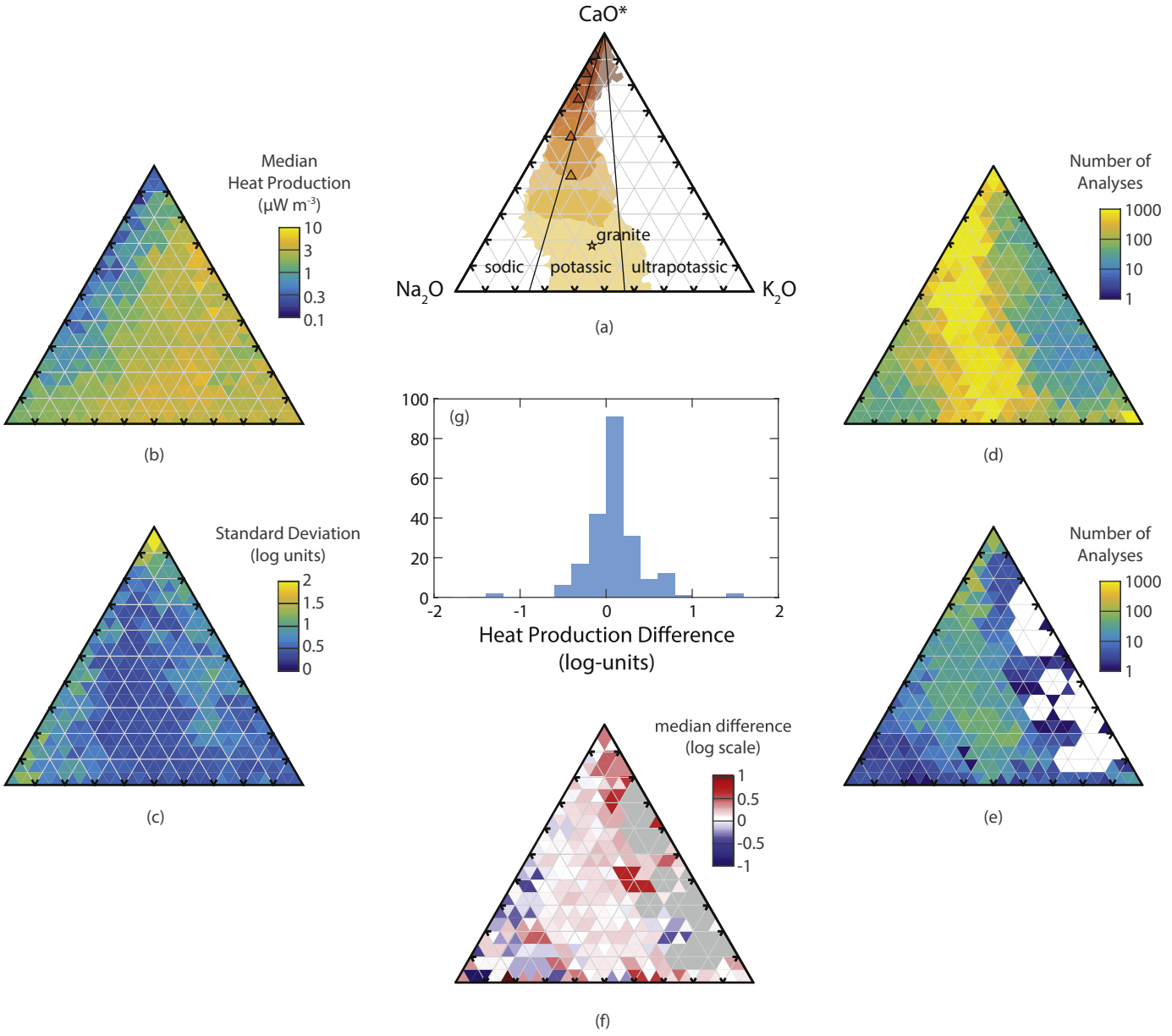

Figure 9. Variations in igneous and metaigneous heat production with CaO^*, Na_2O, and K_2O. Ternary diagrams are computed in molar fraction. CaO^* represents CaO adjusted for apatite (i.e. $n_{CaO^*} = n_{CaO} - 10/3n_{P_2O_5}$, where n is the number of moles). (a) Median points and contours encompassing 90% of subalkaline plutonic rocks defined by the TAS classification (Middlemost, 1994). Samples progress from granite to peridotgabbro. (b) Median heat production and (c) standard deviation ($\log_{10}$ units) for combined igneous and metaigneous samples. Number of (d) igneous and (e) metaigneous samples. (f) Difference between $\log_{10}$ mean of heat production between igneous and metaigneous samples. (g) Histogram of the difference in means.

5. Results and discussion

5.1. Heat production vs. major elements

Two clear observations are apparent from heat production patterns with major oxide concentrations (Fig. 5). First, heat production patterns with major elements are fundamentally different between igneous and sedimentary protoliths (Fig. 5). Second, metamorphic rocks exhibit similar major oxide–heat production patterns with respect to their protoliths.

While the natural variability is very large among the igneous samples, the average behavior is quite well resolved due to the large number of samples (Fig. 5). The heat production of igneous-derived samples increases with SiO_2 and decreases with CaO and more mafic associated elements FeO^t, MgO, and TiO_2 (Fig. 5). The variation in heat production with respect to major oxides in igneous samples is due to the dominant processes that occur during partial melting and fractional crystallization. Since HPEs are incompatible during melting, they tend to increase in concentration at low degrees of partial melt and remain in the melt as it begins to crystallize. Both low degrees of partial melting and crystallization tend to increase the SiO_2 concentration of a melt while decreasing FeO and MgO. As a result felsic rocks tend to have higher heat production whereas mafic rocks tend to have lower heat production. These trends are discussed in greater detail by Hasterok and Webb (2017).

Among sedimentary protoliths, a slight decrease in heat production with SiO_2 above 70 wt.% is observed (Fig. 5). The physical and chemical weathering processes of igneous rocks tends to separate clay-rich from quartz rich sands. As a result, quartz-rich

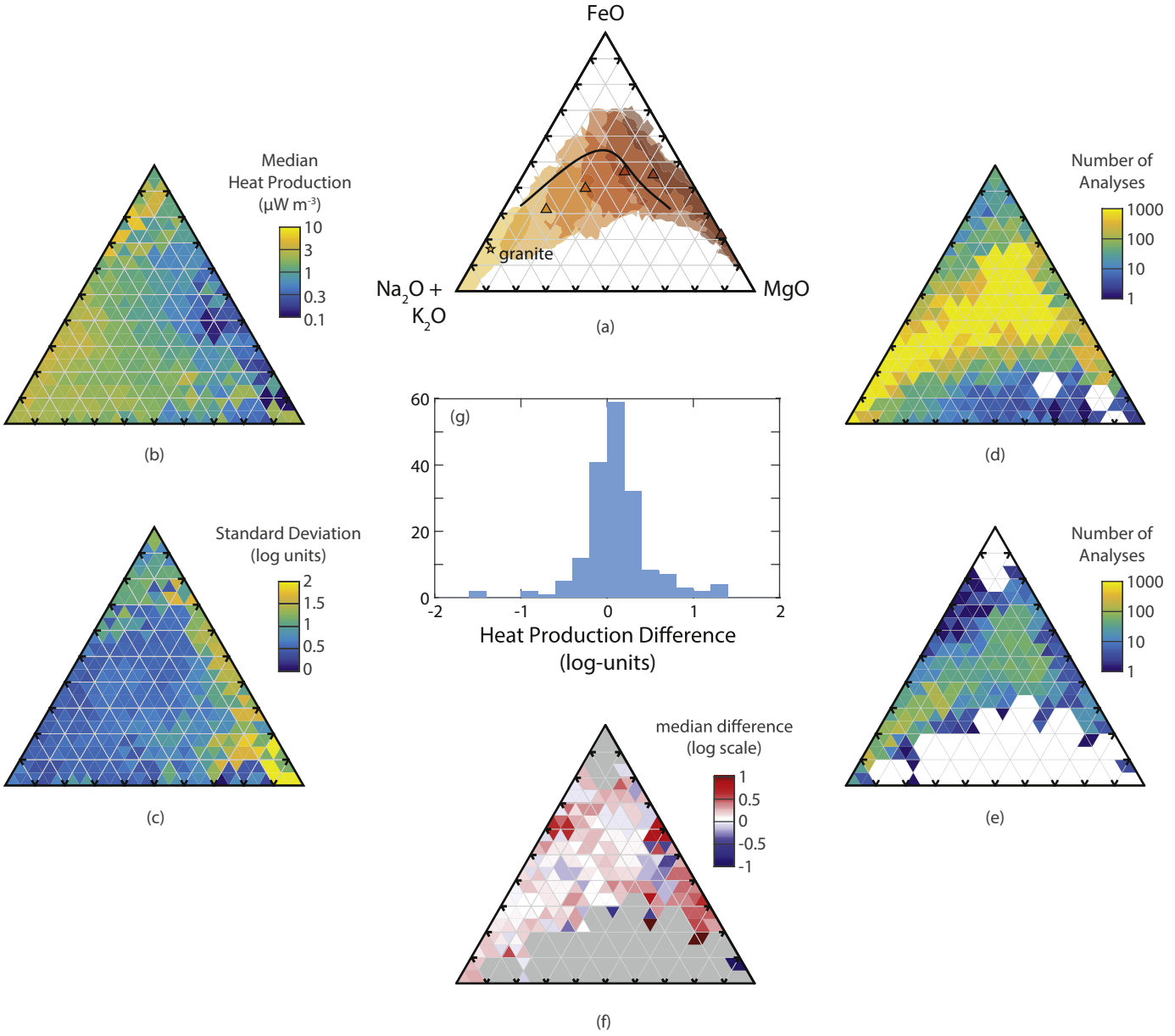

Figure 10. Variations in igneous and metaigneous heat production in the tholeiitic and calc-alkaline system. Ternary diagrams are computed in mass fraction. (a) Median points and contours encompassing 90% of subalkaline plutonic rocks defined by the TAS classification (Middlemost, 1994). Samples progress from granite to peridotgabbro. The solid line indicates the division between tholeiitic (above) and calc-alkaline (below) classification. (b) Median heat production and (c) standard deviation (log_{10} units) for combined igneous and metaigneous samples. Number of (d) igneous and (e) metaigneous samples. (f) Difference between log_{10} mean of heat production between igneous and metaigneous samples. (g) Histogram of the difference in means.

sediments evolve towards pure quartz-arenites (Cox and Lowe, 1995). This purification tends to produce sediments lower heat production than the original rock while increasing the relative mass fraction SiO_2.

Heat production also increases slightly with increasing SiO_2 up to ~65 wt.%. Mixing of sediments derived from mafic igneous rocks and clay-rich sediments derived from felsic igneous rocks may be responsible for the trend in low to moderate SiO_2. Clays produced from felsic rocks tend to have higher K and incompatible trace elements from the source, whereas clays derived from mafic rocks tend to be higher in Ca and Mg and fewer incompatible trace elements.

Heat production within sediments also increases with Al_2O_3, TiO_2, and FeO^t. The increase in heat production with these three chemical components are likely in response to their prevalence in clays (Al) and oxides (Fe, Ti) which are not easily dissolved during the weathering process. These trends differ from igneous-derived sample which show no discernible trend with Al_2O_3 and decreases with TiO_2 and FeO^t. Similar to igneous-derived samples, heat production decreases as CaO increases, but the decrease occurs with a considerably lower slope in the sedimentary data (Fig. 5).

In both igneous- and sedimentary-derived samples heat production increases with K_2O. This observation is unsurprising as K is a heat producing element and is relatively highly correlated to U and Th concentrations.

Both metaigneous and metasedimentary rocks fall within a narrower compositional range than their unmetamorphosed counterparts (Fig. 5), possibly the result of sampling bias. The types of rocks sampled for geochemical and petrological analysis differ depending upon the types of scientific questions posed. While this is unlikely to explain the difference between igneous and sedimentary major oxide patterns, this may explain why metamorphic rocks have narrower compositional ranges. Metamorphic rocks are often selected for phase assemblages that lend themselves to geothermobarometric estimation thus limiting the chemistry of samples selected both between and within lithologic units.

Sedimentary samples have lower natural variability in heat production with respect to igneous samples. This observation most likely results from sedimentary systems integrating multiple sources, effectively averaging the heat production of source units.

5.2. Heat production evolution of metaigneous samples

To examine the compositional variations with heat production in greater depth, we explore the average behavior, variability and differences between igneous and metaigneous samples in three ternary systems (Figs. 8–10). In general, the standard deviations of heat production are $< 0.5\log_{10}$-units within the ternary systems—a considerable improvement over the oxide variograms that are limited to only a single compositional variable (Fig. 5). This suggests that the use of ternary systems improves our ability to understand the variations in HPEs.

Fig. 8 relates variations in heat production to silicic, mafic and potassic components. The common subalkaline rock types (as defined from a TAS diagram) show a progression of increasing SiO_2 from mafic to felsic compositions as well as an increase in K_2O. The range of K_2O values for individual rock types also expand with

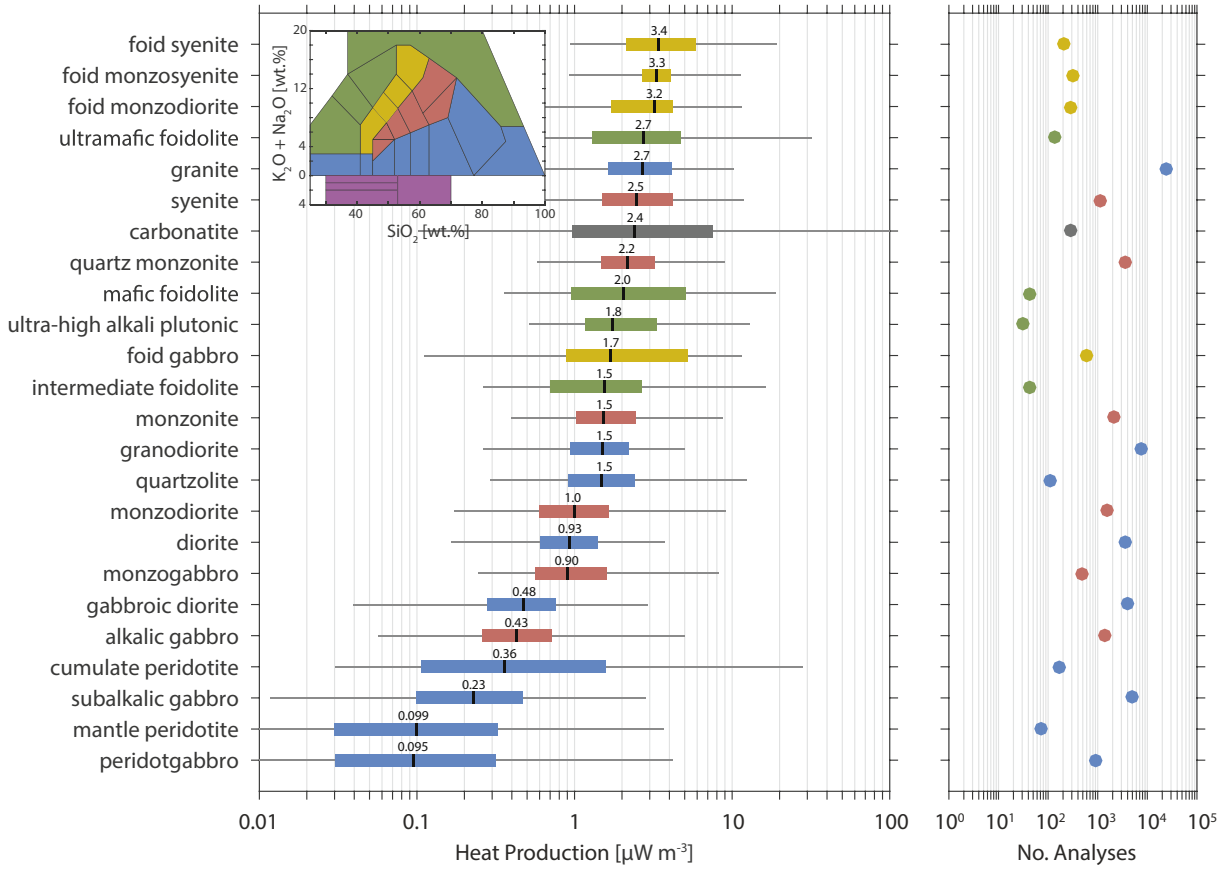

Figure 11. Heat production of plutonic and metaplutonic rocks. The median of each rock is identified by the black vertical line, the box is defined by the 25 to 75 quantiles and the lines indicate the 2.5 to 97.5%. Inset shows TAS scheme used to determine rock type (Middlemost, 1994; Hasterok and Webb, 2017). A table of results are provided in the supplementary material.

increasing SiO_2 (Fig. 8a). Since the TAS fields expand in alkali content as SiO_2 increases it is not surprising to see the rock types on the ternary diagram expand with K_2O.

The largest gradients in heat production occur along the potassic axis and to a lesser degree along the SiO_2 axis when K_2O is held constant (Fig. 8b). The largest increase in heat production from felsic to mafic compositions occur as a result of simultaneous increases in K_2O, which results in the standard view that mafic rocks are low in heat production and felsic rocks are high in heat production. When K_2O is held constant, the observed variations in median heat production increase only slightly as SiO_2 (Fig. 8b). This slight increase occurs because the K/Th ratio decreases as SiO_2 increases, i.e. for constant K_2O, as SiO_2 increases Th also increases slightly increasing heat production. The K/U ratio is relatively constant across all SiO_2 values, therefore, U cannot be responsible for the increase in heat production when K_2O is fixed. An exception to these trends are the high heat producing samples with low SiO_2 and low to moderate K_2O which are dominated by carbonatite compositions.

One of the strongest correlations between geochemical indices and heat production are found with MALI and the feldspar index, which are both defined in terms of CaO, Na_2O and K_2O. The feldspar index includes an additional adjustment to CaO for CaO found in apatite, reducing CaO by 10/3 P_2O_5. In this system, the common igneous rock types begin near the CaO end-member for peridotgabbro. As rocks become more felsic, they become more potassic and progress towards low CaO and nearly equal parts Na_2O as K_2O (Fig. 9a).

Median heat production increases as total alkali, especially K_2O, increases (Fig. 9b). Hence one would expect heat production to be higher in granites rich in K-spar relative to plagioclase. Towards the CaO^* end-member, heat production appears to be influenced almost entirely by the differences in K_2O, irrespective of Na_2O. However, this trend changes as rocks become increasingly alkaline and heat production increases, but is second order with respect to K_2O. The standard deviations are of similar magnitude as observed in Fig. 8c). Standard deviations tend to be highest where the number of data are relatively low.

The previous ternary systems result in larger areas of the plot covered by felsic and intermediate compositions. By examining igneous rocks on an AFM diagram, we can emphasize the mafic end of the compositional spectrum (Fig. 10a). Again the pattern suggests that as rocks become more K_2O rich, they increase in heat production. However, median heat production does not reach values as high as the other two systems. The data also have and higher standard deviations (Fig. 10a and b). The result of this analysis (Fig. 10) is a little more complicated with increasing heat production towards more alkali and tholeiitic compositions. The log-normal scale parameter σ (standard deviation in log-space) is greatest for tholeiitic and more mafic compositions with σ generally >1 to 2 log units. This greater variability may in part be due significantly fewer samples in those areas of the plot. The high heat production values near the FeO^t vertex are the result of carbonatites.

The differences between igneous and metaigneous heat production are generally small for each of the ternary systems,

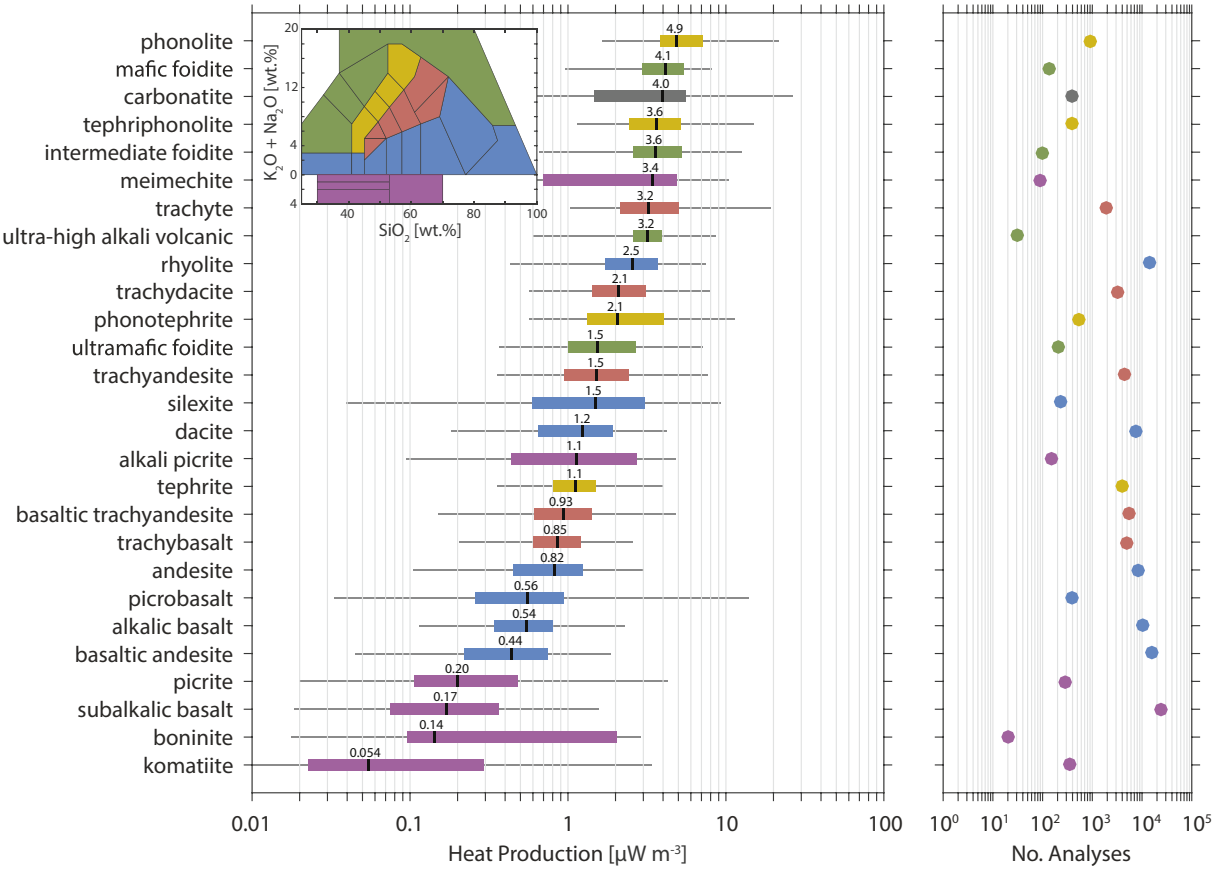

Figure 12. Heat production of volcanic and metavolcanic rocks. The median of each rock is identified by the black vertical line, the box is defined by the 25 to 75 quantiles and the lines indicate the 2.5% to 97.5%. Inset shows TAS scheme used to determine rock type (Middlemost, 1994) with values below the zero line showing fields for high-Mg volcanics with positive total alkali (Le Bas and Streckeisen, 1991). A table of results are provided in the supplementary material.

especially for compositions where the sample numbers are greatest (Figs. 8–10). Aside from the MALI/feldspar system where the difference appears slightly positive for common igneous with respect to metaigneous compositions (Fig. 9f), the differences are generally small <0.2 log units and show relatively little bias towards lower heat production in metaigneous samples with respect to igneous samples (Figs. 8f and 10f). Individually, the largest standard deviations occur where the number of observations are fewest (Fig. 10d and e). Therefore, there is little clear evidence for a difference between samples classified as igneous and metaigneous within the global dataset.

There are two important caveats which may mask any potential systematic difference between igneous and metaigneous samples. First, misclassification of a significant portion of metaigneous samples as igneous samples could reduce an apparent lack of bias by making the two sets of data more similar. Second, it is possible that a spatial sampling bias combined with systematic variations in heat production between disparate regions could result in the apparent lack of difference. These differences vary from region to region and can be significant. For example observed Paleoproterozoic granites in Australia are quite high relative to North American granites (Neumann et al., 2000; McLaren et al., 2003; Hasterok and Webb, 2017).

However, as we will show in Section 5.4, the differences within the metaigneous samples alone as a function of metamorphic grade are quite small and it is reasonable to combine metaigneous and igneous samples to estimate variations in heat production with rock type.

Figs. 11 and 12 show the combined heat production estimates for plutonic and volcanic rock types including metamorphic

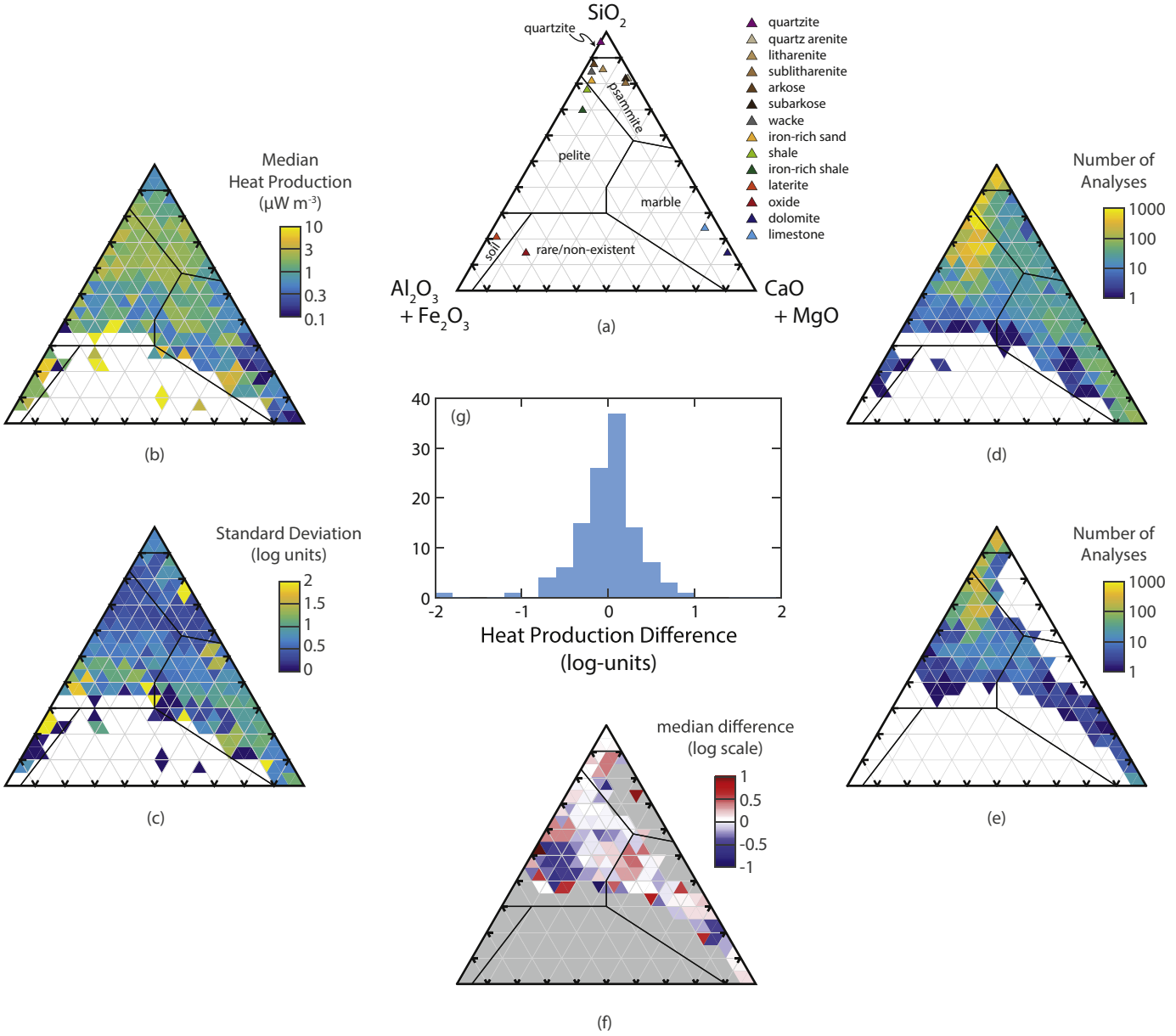

Figure 13. Variations in sedimentary and metasedimentary heat production with rock type and chemistry. Ternary diagrams are computed in mole fraction. (a) Sedimentary rock classification, modified from (Mason, 1952; Turekian, 1969). (b) Median heat production and (c) standard deviation (log_{10} units) for combined sedimentary and metasedimentary samples. Number of (d) sedimentary and (e) metasedimentary samples. (f) Difference between log_{10} mean of heat production between sedimentary and metasedimentary samples. (g) Histogram of the difference in means.

analyses. The results are very similar to our previous model (Hasterok and Webb, 2017) with a few differences resulting from a change in the model used for density estimation and inclusion of several thousand additional data. The largest changes from our previous result occur among highly alkaline and high-Mg igneous rocks which had proportionally larger increases in sample numbers.

5.3. Heat production evolution of metasediments

We examine the heat production of sedimentary rocks in much the same manner as igneous samples above. Using the ternary classification system for sedimentary rocks modified from Mason (1952) and Turekian (1969), we can identify trends in heat production related to the major element chemistry (Fig. 13b). Heat production is highest on average among pelites and decreases with increasing SiO_2 and carbonate (CaO + MgO). Psammites are lower heat production than pelites, but higher than quartzites. Rocks with ~10% or less Al_2O_3 and $Fe_2O_3^t$ have among the lowest heat production for sedimentary samples. Like igneous-derived samples, comparison between sedimentary and metasedimentary samples show little convincing heat production bias between the datasets (Fig. 13f and g).

There is a significant overlap between some of the clastic sedimentary rock types in the SiO_2–$Fe_2O_3^t$ + Al_2O_3–CaO + MgO system. Shales and iron-rich shales are largely contained within the pelite field, but extend into the psammite field. Likewise iron-rich sands are largely contained within a narrow portion of the psammite field, but extend into the pelite field. Examining heat production by rock type reveals additional variations in heat production.

Shales are arguably the most important sedimentary rocks, representing approximately 80% of sedimentary rocks by volume (Clarke and Washington, 1924). The heat production of rocks classified as shale have relatively high heat production on average (2.9 μW m^{-3}) whereas iron-rich shales are more modest heat producing with a median heat production of 1.7 μW m^{-3}. While the compositional range of all shales are quite large, the average compositions are highly skewed to the upper corner of the pelite field (Fig. 13a). The heat production of the interquartile range is relatively narrow in comparison to most other rock types (Fig. 14). Our estimates of heat production are broadly consistent with previous estimates based on chemistry (Wollenberg and Smith, 1987).

Clastic, non-shale sample classified using the (Herron, 1988) system result in narrow, often overlapping and parallel bands perpendicular to the $Fe_2O_3^t$ + Al_2O_3 axis. These rocks fall into two groups, one with lower heat production near the SiO_2–CaO + MgO series (sublitharenite, subarkose, and quartz arenite) and those which fall close to the SiO_2–$Fe_2O_3^t$ + Al_2O_3 series (arkose, iron-rich sand, wacke) with higher heat production (Figs. 13a and 14).

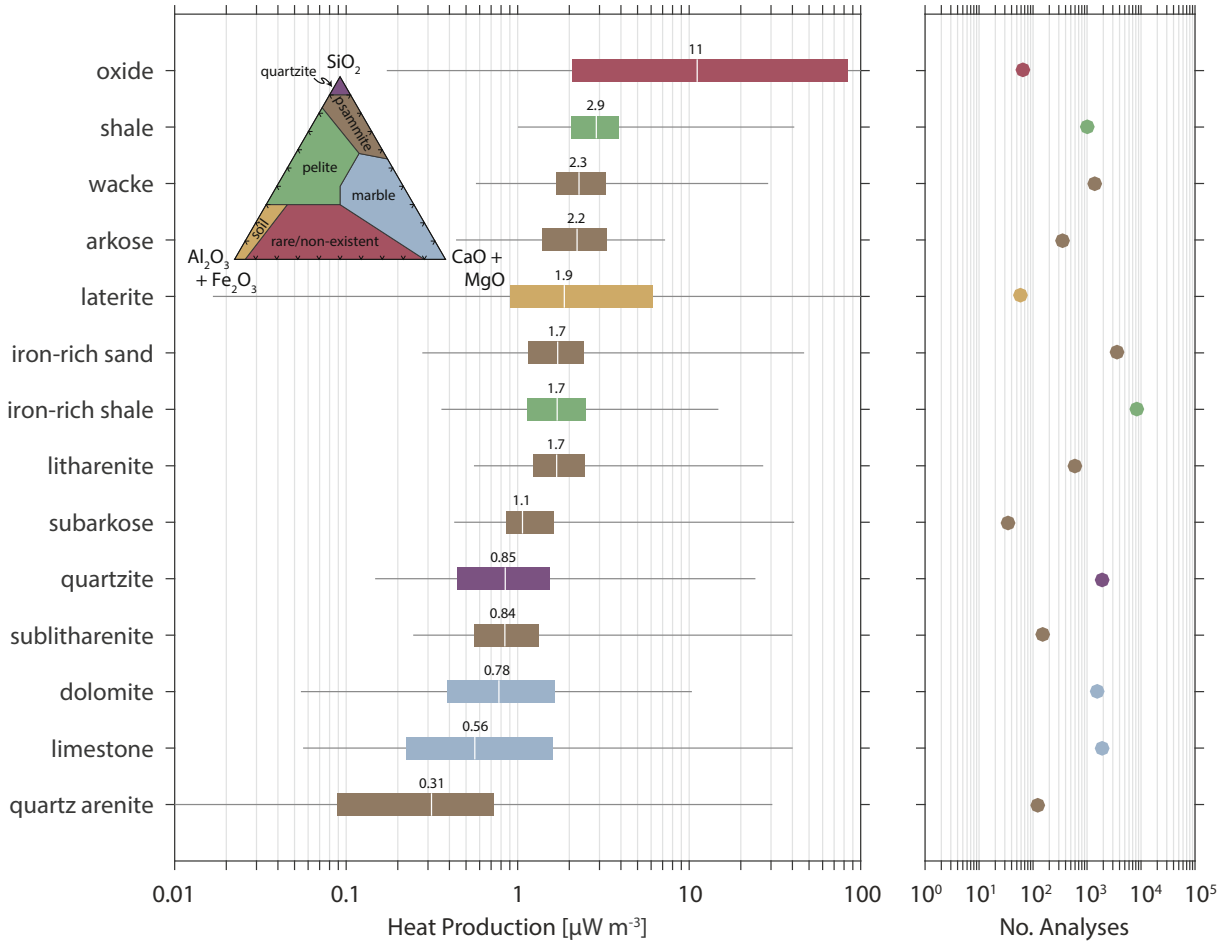

Figure 14. Heat production quantiles for individual sedimentary rock types. Black vertical lines indicate median values, boxes contain 25% to 75% and whiskers indicate 2.5% to 97.5%. The inset images shows the chemical definitions of gross sedimentary rock types used in this study (modified from Mason, 1952; Turekian, 1969). Clastic rock types other than quartzite are determined by (Herron, 1988) and are generally consistent with the general types, but the data distributions do cross the pelite–psammite boundary. A table of results are provided in the supplementary material.

5.4. Heat production versus metamorphic grade

Heat production is generally believed to decrease as a function of increasing metamorphic grade. This existing paradigm is based on three studies of HPEs in metamorphic rocks (Heier and Adams, 1965; Dostal and Capedri, 1978; Bea and Montero, 1999). However, the data supporting these arguments are relatively weak. The study by Heier and Adams (1965) examines 20 granulite samples, but does not control for stratigraphic unit. The three order magnitude variation make it difficult to accept their result on statistical grounds. The study by Dostal and Capedri (1978) is better designed, sampling four stratigraphic units exposed to variations in the metamorphic grade. However the sample numbers are still relatively small. In their study, they suggest that U is unaffected by metamorphism below granulite facies and within granulite facies, U loss may not occur in common accessory phases such as zircon, which contains the bulk of U in most rocks (Dostal and Capedri, 1978). The third study by Bea and Montero (1999) likewise examines very few samples across several units and metamorphic grades (36 samples in total: 16 metasedimentary, 9 metaigneous, and 11 leucosomes from the same units). It is difficult to see how any of these studies can be definitive given the large natural variability in trace elements and limited number of samples analyzed.

There is a decrease in heat production with SiO_2 for all metamorphic conditions for igneous rocks, but the differences with grade for rocks of similar SiO_2 do not show any consistent pattern (Fig. 15a). In some cases there are too few data to make an accurate determination of the heat production distribution.

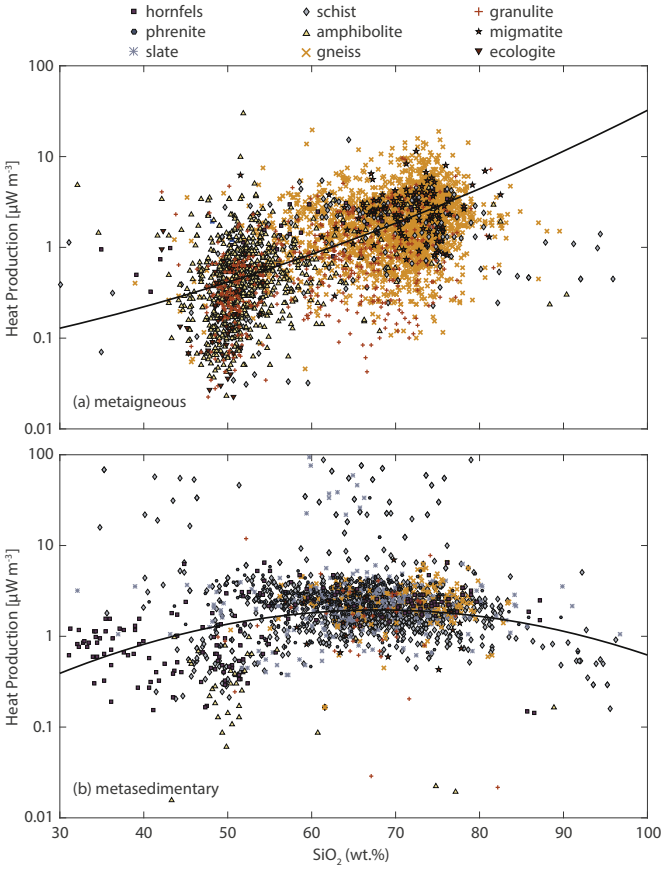

Figure 15. Heat production as a function of SiO_2 content for (a) metaigneous and (b) metasedimentary samples as a function of metamorphic grade. Black curves are quadratic fit to heat production of igneous and sedimentary rocks, respectively. For igneous rocks, the fit is constrained to $40 \leq SiO_2$ (wt.%) ≤ 80; and for sedimentary rocks, the fit is constrained to $30 \leq SiO_2$ (wt.%) ≤ 100.

There is also very little change in heat production of metasedimentary samples with metamorphic grade (Fig. 15b). The distributions of phrenites, schist, granulite and migmatites of metasedimentary origin are all very similar. Each are consistent with the distribution of clastic and clay-rich sediments. Amphibolites have lower heat production, but these rocks have systematically lower SiO_2 than the other facies. The lower SiO_2 values may indicate partial melting has occurred, at which point zircons may dissolve or be removed during melt extraction (Rubatto et al., 2001). Or the lower heat production may simply reflect an application of the term amphibolite to mafic samples whereas felsic samples under amphibolite conditions are more commonly referred to as gneisses. The overlapping heat production distributions for the different metamorphic grades are independent of SiO_2 concentrations. In fact, metasedimentary schists, gneisses, hornfels, and possibly granulites show a slight increase in average heat production with decreasing SiO_2.

The differences between metamorphic grades are obscured by the general pattern of heat production with respect to SiO_2. To remove the effect of SiO_2, we fit a second order polynomial to heat production as a function of SiO_2 (Fig. 15). Rather than fit to the sparse metamorphic data, we fit the trends to igneous and sedimentary data. This curve fit may then be used to detrend the metamorphic data for SiO_2. Once detrended, the heat production observations for each metamorphic grade may be analyzed as a single distribution to compare with another (Fig. 16).

Accounting for a general decrease in SiO_2, there appears to be no clear systematic trend in the median or distribution with respect to grade (Fig. 16). The only potential exceptions to these observations are metaigneous eclogites and metasedimentary amphibolites. The eclogites in this dataset are typically derived from oceanic basalts, which are depleted in HPEs with respect to continental basalts (Hasterok, 2013). It is unclear why the sedimentary amphibolites are low heat producing as they come from a variety of sources.

In light of these observations, we suggest that heat production changes very little with respect to metamorphic grade contrary to the existing paradigm. These observations makes some sense when one considers that it would not be possible to determine protolith ages if the common host minerals for U and Th (zircon and monazite, respectively) were completely removed through metamorphic processes (including high temperatures) (e.g., Chen et al., 2010; Santosh et al., 2016; Waizenhöfer and Massonne, 2017). Indeed several studies of prograde metamorphism in the presence of some metamorphic assemblages can grow accessory monazite as a result of reactions between common silicate minerals (Rubatto et al., 2001; Kohn and Malloy, 2004). Zircon may dissolve under some conditions, but reprecipitate during retrograde paths (Chen et al., 2010; Kohn et al., 2015). Whether U is lost, gained or unchanged depends upon dissolution and precipitation which are influenced by the presence of fluids (including melt), the oxygen fugacity of the fluids, and the relative openness of a system (Rubatto et al., 2001; Baldwin, 2015). Our results may indicate that metamorphic systems are generally more closed than open.

If our interpretations are correct, we suggest that any decrease in heat production with depth is not due to an increases in metamorphic grade, but simply the intrinsic heat production of the protolith itself. To obtain such low heat production as typically quoted for the middle to lower crust ($\sim$0.4 μW m^{-3}, e.g., Hasterok and Chapman, 2011; Jaupart et al., 2016), the proportion of mafic igneous rocks must be relatively high. This is because intermediate and felsic igneous rocks and nearly all compositions of sedimentary rocks are generally too heat producing to result in such low average values.

Further studies that examine the heat production of continuous stratigraphic units that vary considerably with metamorphic grade

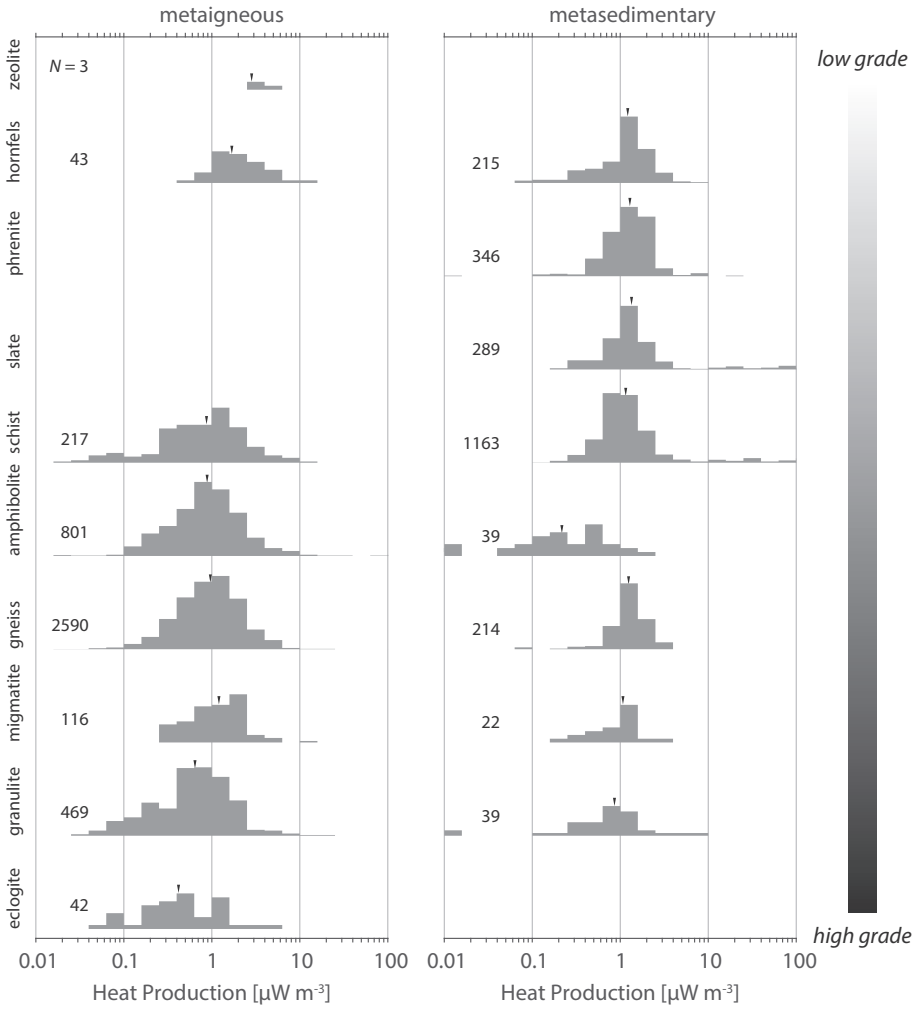

Figure 16. SiO_2-detrended heat production of metaigneous and metasedimentary samples as a function of metamorphic grade. The little arrows over each distribution represent the median heat production.

are required to verify these interpretations. The units must be carefully selected such that the protolith was initially compositionally homogeneous. Future studies must be constructed such that they analyze a large number of samples collected within each metamorphic grade (we recommend a few hundred at each P-T condition) to produce reliable estimates of average heat production in the presence of large natural variability.

6. Conclusions

Our ability to accurately and precisely estimate temperatures within the lithosphere require improved models of heat production and their variability for a wide range of rock types. In this study, we find that the heat production of metamorphic rocks are controlled by the heat production of the protolith. Counter to the prevailing paradigm, we find little convincing evidence for a significant decrease in heat production as a function of metamorphic grade. This observation suggests that metamorphic rocks that have low heat production started with low heat production. An exception would be in the event that melting significantly alters the chemistry of the unmelted rock, but this is self-evident.

The heat production of sedimentary and igneous protoliths have distinctly different patterns of heat production variations with respect to major elements. Within igneous protoliths, heat production increases as a function of SiO_2 and decreases with FeO^t, MgO, CaO and TiO_2. Sedimentary protoliths show a more complex variation in heat production with SiO_2 and increase in heat production with Al_2O_3, FeO^t, and TiO_2. There is a decrease in heat production with increasing CaO. Both sedimentary and igneous protoliths increase in heat production with K_2O.

Furthermore, heat production of sedimentary protoliths fall within a significantly smaller range than that of igneous protoliths. A decrease in heat production that is expected on the basis of thermal constrains suggests that the lower crust must be igneous rather than sedimentary. However, local and regional deep burial of sedimentary protoliths could have profound implications on the thermal state of the crust and, as a consequence, the potential for radiogenically induced melting and internal deformation.

Acknowledgements

We would like to thank the Associate Editor Dr. Chris Spencer and Trond Slagstad for helpful reviews. We would like to thank the following for providing datasets and/or personal compilations: D. Champion (GA), D. Claeson (SGU), T. Slagstad (NGU), and H. Furness. Peter Johnson provided a collection of papers with data for the Arabian-Nubian Shield. DH would like to thank Philip Dixon for a helpful discussion about data censoring. M. Gard is supported by Australian Government Research Training Program Scholarship.

Appendix A. Supplementary data

Supplementary data related to this article can be found at https://doi.org/10.1016/j.gsf.2017.10.012.

References

Baldwin, S.L., 2015. Zircon dissolution and growth during metamorphism. American Mineralogist 100, 1019–1020. https://doi.org/10.2138/am-2015-5279.

Barette, F., Poppe, S., Smets, B., Benbakkar, M., Kervyn, M., 2016. Spatial variation of volcanic rock geochemistry in the Virunga Volcanic Province: statistical analysis of an integrated database. Journal of African Earth Sciences. https://doi.org/10.1016/j.jafrearsci.2016.09.018.

Bea, F., Montero, P., 1999. Behavior of accessory phases and redistribution of Zr, REE, Y, Th, and U during metamorphism and partial melting of metapelites in the lower crust: an example from the Kinzigite Formation of Ivrea-Verbano, NW Italy. Geochimica et Cosmochimica Acta 63, 1133–1153. https://doi.org/10.1016/s0016-7037(98)00292-0.

Bédard, J.H., Hayes, B., Hryciuk, M., Beard, C., Williamson, N., Dell'Oro, T.A., Rainbird, R.H., Prince, J., Baragar, W.R.A., Nabelek, P.I., Weis, D., Wing, B., Scoates, J., Naslund, H.R., Cousens, B., Williamson, M.C., Hulbert, L.J., Montjoie, R., Girard, É., Ernst, R., Lissenberg, C.J., 2016. Geochemical database of Franklin sills, Natkusiak basalts and shaler Supergroup rocks, Victoria Island, Northwest Territories, and correlatives from Nunavut and the mainland. Open-file 8009. Geological Survey of Canada. https://doi.org/10.4095/297842.

Boyd, F.R., McCallister, R.H., 1976. Densities of fertile and sterile garnet peridotites. Geophysical Research Letters 3, 509–512. https://doi.org/10.1029/gl003i009p00509.

Chen, R.X., Zheng, Y.F., Xie, L., 2010. Metamorphic growth and recrystallization of zircon: distinction by simultaneous in-situ analyses of trace elements, U–Th–Pb and Lu–Hf isotopes in zircons from eclogite-facies rocks in the Sulu orogen. Lithos 114, 132–154. https://doi.org/10.1016/j.lithos.2009.08.006.

Christensen, N., Mooney, W., 1995. Seismic velocity structure and composition of the continental crust: a global view. Journal of Geophysical Research 100, 9761–9788. https://doi.org/10.1029/95JB00259.

Clarke, F., Washington, H., 1924. The Composition of the Earth's Crust. Professional Paper 127. USGS.

Cox, R., Lowe, D., 1995. A conceptual review of regional-scale controls on the composition of clastic sediment and the co-evolution of continental blocks and their sedimentary cover. Journal of Sedimentary Research A65, 1–12.

Dostal, J., Capedri, S., 1978. Uranium in metamorphic rocks. Contributions to Mineralogy and Petrology 66, 409–414. https://doi.org/10.1007/bf00403426.

Hasterok, D., 2013. A heat flow based cooling model for tectonic plates. Earth and Planetary Science Letters 361, 34–43. https://doi.org/10.1016/j.epsl.2012.10.036.

Hasterok, D., Chapman, D., 2011. Heat production and geotherms for the continental lithosphere. Earth and Planetary Science Letters 307, 59–70. https://doi.org/10.1016/j.epsl.2011.04.034.

Hasterok, D., Webb, J., 2017. On the radiogenic heat production of igneous rocks. Geoscience Frontiers 8, 919–940. https://doi.org/10.1016/j.gsf.2017.03.006.

Haus, M., Pauk, T., 2010. Data from the PETROCH lithogeochemical database. Miscellaneous release—data 250. Ontario Geological Survey.

Heier, K., Adams, J., 1965. Concentration of radioactive elements in deep crustal material. Geochimica et Cosmochimica Acta 29, 53–61. https://doi.org/10.1016/0016-7037(65)90078-5.

Helsel, D.R., 2004. Nondetects and Data Analysis: Statistics for Censored Environmental Data. J. Wiley & Sons. URL: http://www.ebook.de/de/product/5530994/dennis_r_helsel_usgs_dennis_r_heisel_nondetects_and_data_analysis_statistics_for_censored_environmental_data.html.

Herron, M.M., 1988. Geochemical classification of terrigenous sands and shales from core or log data. SEPM Journal of Sedimentary Research 58. https://doi.org/10.1306/212f8e77-2b24-11d7-8648000102c1865d.

Jaupart, C., Mareschal, J.C., Iarotsky, L., 2016. Radiogenic heat production in the continental crust. Lithos 262, 398–427. https://doi.org/10.1016/j.lithos.2016.07.017.

Jeanniot, L., Kusznir, N., Mohn, G., Manatschal, G., Cowie, L., 2016. Constraining lithosphere deformation modes during continental breakup for the Iberia–Newfoundland conjugate rifted margins. Tectonophysics 680, 28–49. https://doi.org/10.1016/j.tecto.2016.05.006.

Kelsey, D., Hand, M., 2015. On ultrahigh temperature crustal metamorphism: phase equilibria, trace element thermometry, bulk composition, heat sources, timescales and tectonic settings. Geoscience Frontiers 6, 311–356. https://doi.org/10.1016/j.gsf.2014.09.006.

Kirkland, C., Smithies, R., Taylor, R., Evans, N., McDonald, B., 2015. Zircon Th/U ratios in magmatic environs. Lithos 212–215, 397–414. https://doi.org/10.1016/j.lithos.2014.11.021.

Kohn, M.J., Corrie, S.L., Markley, C., 2015. The fall and rise of metamorphic zircon. American Mineralogist 100, 897–908. https://doi.org/10.2138/am-2015-5064.

Kohn, M.J., Malloy, M.A., 2004. Formation of monazite via prograde metamorphic reactions among common silicates: implications for age determinations. Geochimica et Cosmochimica Acta 68, 101–113. https://doi.org/10.1016/s0016-7037(03)00258-8.

Laske, G., Masters, G., 1997. A global digital map of sediment thickness. Eos Transactions American Geophysical Union 78, F483.

Le Bas, M., Streckeisen, A., 1991. The IUGS systematics of igneous rocks. Journal of the Geological Society of London 148, 825–833.

Liu, S., Currie, C.A., 2016. Farallon plate dynamics prior to the Laramide Orogeny: numerical models of flat subduction. Tectonophysics 666, 33–47. https://doi.org/10.1016/j.tecto.2015.10.010.

Mason, B., 1952. Principles of Geochemistry. J Wiley & Sons.

McDonough, W.F., Arevalo, R., 2008. Uncertainties in the composition of Earth, its core and silicate sphere. Journal of Physics: Conference Series 136, 022006. https://doi.org/10.1088/1742-6596/136/2/022006.

McKenzie, D., Priestley, K., 2016. Speculations on the formation of cratons and cratonic basins. Earth and Planetary Science Letters 435, 94–104. https://doi.org/10.1016/j.epsl.2015.12.010.

McLaren, S., Sandiford, M., Hand, M., Neumann, N., Wyborn, L., Bastrakova, I., 2003. The hot south continent: heat flow and heat production in Australian Proterozoic terranes. Geological Society of Australia Special Publication 22, 151–161. https://doi.org/10.1130/0-8137-2372-8.157.

McLaren, S., Sandiford, M., Powell, R., Newmann, N., Woodhead, J., 2006. Palaeozoic intraplate crustal anatexis in the Mount Painter Province, South Australia: timing, thermal budgets and the role of crustal heat production. Journal of Petrology 47, 2281–2302.

Middlemost, E., 1994. Naming materials in the magma/igneous rock system. Earth-Science Reviews 37, 215–224. https://doi.org/10.106/0012-8252(94)90029-9.

Neumann, N., Sandiford, M., Foden, J., 2000. Regional geochemistry and continental heat flow: implications for the origin of the South Australian heat flow anomaly. Earth and Planetary Science Letters 183, 107–120. https://doi.org/10.1016/S0012-821X(00)00268-5.

Rubatto, D., Williams, I.S., Buick, I.S., 2001. Zircon and monazite response to prograde metamorphism in the Reynolds range, central Australia. Contributions to Mineralogy and Petrology 140, 458–468. https://doi.org/10.1007/pl00007673.

Rybach, L., 1988. Determination of heat production rate. In: Hänel, R., Rybach, L., Stegena, I. (Eds.), Terrestrial Handbook of Heat-flow Density Determination. Kluwer Academic Publishers, Dordrecht, pp. 125–142. Chapter 4.2.

Sandiford, M., Hand, M., McLaren, S., 2001. Tectonic feedback, intraplate orogeny and the geochemical structure of the crust: a central Australian perspective. In: Miller, J., Holdsworth, J., Buick, I., Hand, M. (Eds.), Continental Reactivation and Reworking, vol. 184. Geol. Soc., London, pp. 195–218. Spec. Pub.

Santosh, M., Yang, Q.Y., Shaji, E., Mohan, M.R., Tsunogae, T., Satyanarayanan, M., 2016. Oldest rocks from peninsular India: evidence for Hadean to Neoarchean crustal evolution. Gondwana Research 29, 105–135. https://doi.org/10.1016/j.gr.2014.11.003.

Sizova, E., Gerya, T., Stwe, K., Brown, M., 2015. Generation of felsic crust in the Archean: a geodynamic modeling perspective. Precambrian Research 271, 198–224. https://doi.org/10.1016/j.precamres.2015.10.005.

Slagstad, T., 2008. Radiogenic heat production of Archean to Permian geological provinces in Norway. Norwegian Journal of Geology 88, 149–166.

Slagstad, T., 2017. LITO Database (Online): Geochemical Mapping of Norwegian Bedrock. Technical Report. Norges Geologiske Undersøkele (NGU). URL: http://www.ngu.no/lito.

Taylor, S., McLennan, S., 1985. The Continental Crust: Its Composition and Evolution. Blackwell, Oxford.

Toft, P.B., Arkani-Hamed, J., Haggerty, S.E., 1990. The effects of serpentinization on density and magnetic susceptibility: a petrophysical model. Physics of the Earth and Planetary Interiors 65, 137–157. https://doi.org/10.1016/0031-9201(90)90082-9.

Turekian, K., 1969. The oceans, streams and atmosphere. In: Handbook of Geochemistry, vol. 1. Springer-Verlag Berlin, Heidelberg, New York, pp. 297–323.

Waizenhöfer, F., Massonne, H.J., 2017. Monazite in a Variscan mylonitic paragneiss from the Mnchberg metamorphic complex (NE Bavaria) records Cadomian protolith ages. Journal of Metamorphic Geology 35, 453–469. https://doi.org/10.1111/jmg.12240.

Wilkinson, B.H., McElroy, B.J., Kesler, S.E., Peters, S.E., Rothman, E.D., 2009. Global geologic maps are tectonic speedometers—rates of rock cycling from area-age frequencies. Geological Society of America Bulletin 121, 760–779. https://doi.org/10.1130/b26457.1.

Wollenberg, H., Smith, A., 1987. Radiogenic heat production of crustal rocks: an assessment based on geochemical data. Geophysical Research Letters 14, 295–298. https://doi.org/10.1029/gl014i003p00295.